Theses and Dissertations
Theses, Dissertations, and Senior Projects

1-1-2017

Parkinson's Symptoms quantification using wearable sensors

Md Nafiul Alam

Parkinson's Symptoms Quantification Using Wearable Sensors

by

Md Nafiul Alam
Bachelor of Science, Khulna University of Engineering and Technology

A Thesis

Submitted to the Graduate Faculty

of the

University of North Dakota

in partial fulfillment of the requirements

for the degree of

Master of Science

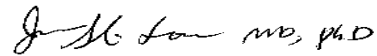Grand Forks, North Dakota
December
2017

This thesis, submitted by Md. Nafiul Alam in partial fulfillment of the requirements for the Degree of Master of Science from the University of North Dakota, has been read by the Faculty Advisory Committee under whom the work has been done and is hereby approved.

_____

Dr. Reza Fazel-Rezai

_____

Dr. Kouhyar Tavakolian

_____

Dr. Jau-Shin Lou

_____

Dr. Colin Combs

This thesis is being submitted by the appointed advisory committee as having met all of the requirements of the School of Graduate Studies at the University of North Dakota and is hereby approved.

_____

Grant McGimpsey,
Dean of the Graduate School

_____

Da

PERMISSION

Title   Parkinson's Symptoms Quantification Using Wearable Sensors.

Department   Electrical Engineering

Degree   Master of Science

    In presenting this thesis in partial fulfillment of the requirements for a graduate degree from the University of North Dakota, I agree that the library of this University shall make it freely available for inspection. I further agree that permission for extensive copying for scholarly purposes may be granted by the professor who supervised my thesis work or, in his absence, by the chairperson of the department or the dean of the Graduate School. It is understood that any copying or publication or other use of this thesis or part thereof for financial gain shall not be allowed without my written permission. It is also understood that due recognition shall be given to me and to the University of North Dakota in any scholarly use which may be made of any material in my thesis.

Md. Nafiul Alam
November 18th , 2017

TABLE OF CONTENTS

Contents

LIST OF FIGURES

LIST OF TABLES

ACKNOWLEDGEMENTS

ABSTRACT

Parkinson's disease (PD) is a common neurodegenerative disorder affecting more than one million people in the United States and seven million people worldwide. Motor symptoms such as tremor, slowness of movements, rigidity, postural instability, and gait impairment are commonly observed in PD patients. Currently, Parkinsonian symptoms are usually assessed in clinical settings, where a patient has to complete some predefined motor tasks. Then a physician assigns a score based on the United Parkinson's Disease Rating Scale (UPDRS) after observing the motor task. However, this procedure suffers from inter subject variability. Also, patients tend to show fewer symptoms during clinical visit, which leads to false assumption of the disease severity. The objective of this study is to overcome this limitations by building a system using Inertial Measurement Unit (IMU) that can be used at clinics and in home to collect PD symptoms data and build algorithms that can quantify PD symptoms more effectively. Data was acquired from patients seen at movement disorders Clinic at Sanford Health in Fargo, ND. Subjects wore Physilog IMUs and performed tasks for tremor, bradykinesia and gait according to the protocol approved by Sanford IRB. The data was analyzed using modified algorithm that was initially developed using data from normal subjects emulating PD symptoms. For tremor measurement, the study showed that sensor signals collected from the index finger more accurately predict tremor severity compared to signals from a sensor placed on the wrist.

For finger tapping, a task measuring bradykinesia, the algorithm could predict with more than 80% accuracy when a set of features were selected to train the prediction model. Regarding gait, three different analysis were done to find the effective parameters indicative of severity of PD. Gait speed measurement algorithm was first developed using treadmill as a reference. Then, it was shown that the features selected could predict PD gait with 85.5% accuracy.

CHAPTER 1

INTRODUCTION

1.1 Motivation

Since I started my education in Electrical Engineering, it has always been my utmost desire to use the knowledge I gained to improve human health and quality of life. Some fascinating discovery in technology over the years to solve human health issue have inspired me to work and contribute on this area. From our early life, we have been exposed to different medical device system (e.g., X-Ray, Magnetic resonance imaging (MRI), Electrocardiogram (ECG), a smart blood glucose meter). Whenever I encountered with those technologies, I always got intrigued about how the system operates or what the internal mechanism of the system is. Path-breaking advances have been made to diagnose different critical disease using technology. However, assessing the severity of Parkinson's Disease (PD) objectively remains a challenge. Very few devices have been introduced to diagnose and monitor PD and symptoms. By personally observing the sufferings of PD patient, I decided to dig deep into the possible solutions for diagnosing and monitoring PD symptoms using technology.

1.2 Parkinson's Disease (PD)

PD is a disorder of the nervous system, which is the result of the loss of brain cells that are responsible for the production of dopamine [1]. The disease affects the movement of the people suffering the from it. The primary symptoms of PD are 1) tremor, or shaking of different body

parts; 2) rigidity or stiffness of the muscles and trunk; 3) bradykinesia or slowness of movement; and 4) postural instability, or impaired balance and coordination. As these symptoms become more prominent, patients may face trouble during walking, talking or completing any simple errands. PD usually affects older people with age over 60 years old [2]. Usually, early symptoms are not much noticeable and it progresses gradually. The rate of progression of the disease is patient specific as it may spread faster in some patients compared to others. As the disease progresses, the tremor symptoms, which affects most of the people with PD may begin to cause difficulties in doing daily activities. PD patients usually suffer from non-motor symptoms that may include depression and anxiety disorder; hardship in eating and speaking; constipation; skin disease; and sleep disorder [3].

Almost one million people in United States are suffering from PD [4]. Each year, approximately 60,000 Americans are diagnosed with PD each year. Actual number might be more as thousands of numbers go undetected which do not reflect in the overall numbers. Worldwide, almost 10 million people are living with PD. Although, occurrence of PD rises with age, as high as four percent of the PD patients are diagnosed before the age of 50. Another important statistic is that men are one and a half times more likely to diagnose with PD than women [4]. There is a direct and indirect cost associated with the various aspect of PD such as treatment, payments regarding social security and lost income from inability to work. The whole price in the United States alone estimated to be approximately $25 billion per year [1].
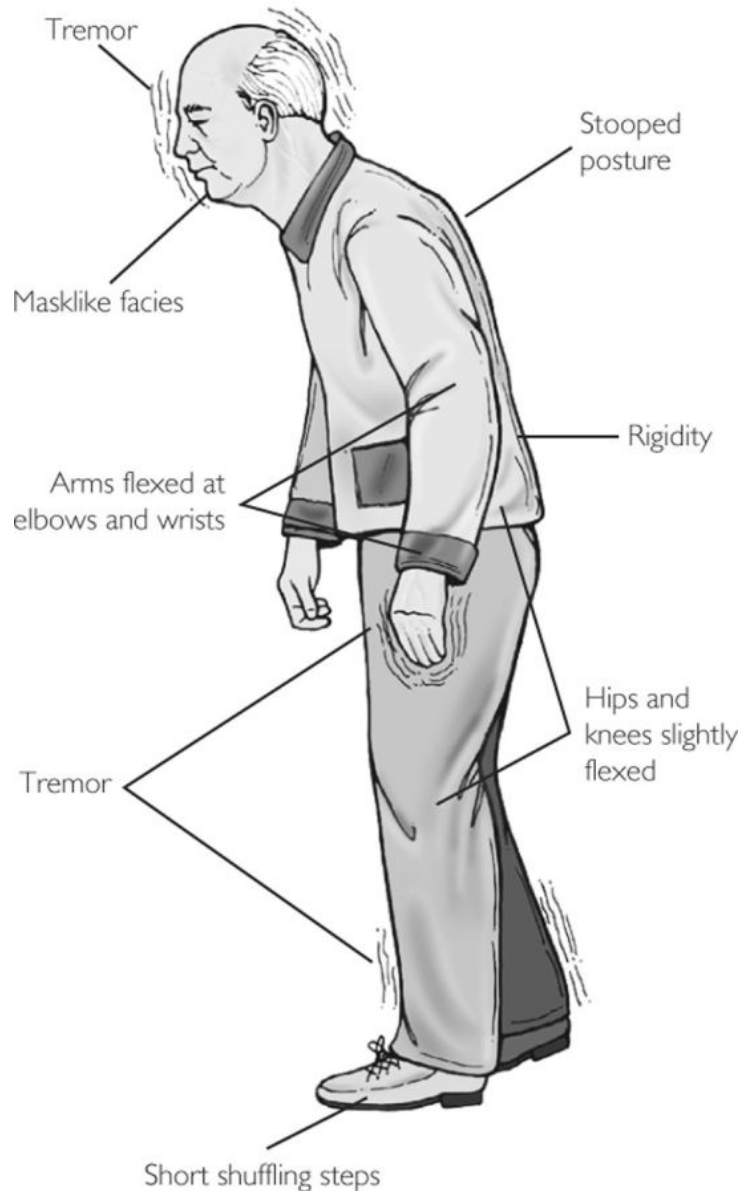
Figure 1. Parkinson's disease symptoms [5]

The disease develops gradually but usually starts with a low severity tremor in just one hand [3]. It also causes rigidity and slowness of movement in the patient. There are several signs occurred in people suffering from early stages of PD disease. The face of the subject may show little or no expression, or exhibit reduces arm swing during walking. Speech may be distorted to become soft or slurred. PD symptoms worsen as your condition progresses over time. PD is a chronic disease. A variety of medications can control and reduce the effects of the symptoms but,

the disease is not curable at the moment [6]. Usually, levodopa in combination with carbidopa is generally given to affected PD patients [7][8]. Carbidopa delays the conversion of levodopa into dopamine until it reaches the brain [7]. Levodopa improves the nerve cells ability to produce dopamine and restores the brain's dwindling supply. Although levodopa helps at least three-quarters of PD cases, not all symptoms respond equally to the drug [7]. Among the primary symptoms, bradykinesia and rigidity respond better, while tremor symptoms effect may be slightly reduced. However, the levodopa may not improve balance and other symptoms at all. In some cases, Deep Brain Stimulation surgery approved by the U.S. Food and Drug Administration may be the right choice if the disease doesn't respond to medication [9]. In DBS, doctor implant electrodes into the brain. Electrodes are connected to a tiny electrical device called a pulse generator that can be programmed [10]. DBS can lower the need for levodopa and similar drugs, thus reducing the side effect (e.g., dyskinesia) associated with those medicines. DBS requires cautious programming of the stimulator device to work correctly. In occasional cases, doctor may suggest surgery to regulate specific regions of the brain and improve PD symptoms.

In this study, we have investigated three main PD symptoms which are tremor, bradykinesia and gait described as follows.

1.2.1   Tremor

Tremor in hand is the most noticeable feature in PD. In early stages of the disease, almost 70% of patients show signs of tremor or shaking in one hand or one foot on one side of the body [11] . PD patients exhibit different types of tremor. Usually, tremor in rest is most predominant type of tremor happens in PD patients. Rest tremor has average amplitude and frequency range in 3.5-7.5 Hz [12]. Postural tremor is another types of tremor which can be tested on PD patients where subjects required to hold their hand outstretched which also has a dominant frequency in range

same as rest tremor. Essential tremor which is not PD tremor may have frequency in the range 4-12 Hz [13]. Action tremor is less frequent in PD patients. Many PD patients experience less severe tremor while actually using their hands to do something. This characteristic is actually opposite of essential tremor which is more dominant in the active state of the limbs.

Figure 2. Rest and postural tremor [14]**. Subjects on left hand side is performing resting tremor tasks. Subjects on the right is performing postural tremor task.**

The pathophysiology of resting tremor is mostly unknown, but evidence suggests that it differs from that of bradykinesia symptoms [15]. It is known that severely affected side of rest tremor can be opposite to the bradykinesia affected side. Also, the intensity of shaking is not related to dopamine deficiency [16]. Some study indicates a role of dopaminergic loss in the midbrain retrorubral A8 region, which points to the pallidum and is separate from the nigrostriatal pathways, is the origin of rest tremor [15]. It was also found that the severity of rest tremor correlated with a decrease in median raphe serotonin receptor binding [17]. The finding suggests that serotoninergic neuron loss might be more closely connected to the focalization of this symptom. However, serotoninergic drugs do not usually improve tremor in PD which makes the above finding controversial [16].

1.2.2 Bradykinesia

Bradykinesia is the primary symptom of PD [3]. It causes slowness of movement in patients [18]. PD patients with these symptoms faces difficulties in preparing, originating and executing movements. The initial sign includes slowness in performing activities of daily living and slow reaction times. The usually greater difficulty lies with tasks that require fine motor controls, e.g., buttoning. Bradykinesia may cause a person to take shuffling steps and have a problem with walking. Other manifestations of bradykinesia include reduction of facial expression, drooling due to impaired swallowing, decreasing eye blink rate and reduced arm swing during walking [18].

The person with advanced bradykinesia may feel that are unable to move their feet as they think the body would not respond to their brain. The emotional state of a PD patient may also change bradykinesia symptoms. It is observed that people with bradykinesia sometimes respond well in emergency cases like in case of fire they may get up and run [17]. This phenomenon suggests that PD patients may have motor programs undamaged but having difficulty retrieving them.

The pathophysiology behind this symptom is not completely understood. However, much significant research has been done to understand the mechanism of bradykinesia symptoms. According to the classical model of the prevalence of the indirect pathway to the direct ones in BG [19] [20], initiation of the movement or its execution may be affected by the failure of the BG output to support the cortical mechanisms. EEG studies have shown abnormalities in pre-movement potential in PD patients. Causes of bradykinesia were also investigated by Dick et al. [21]. His research shows bradykinesia or slower movement is related to a slower increase in cortical excitability before movement [21].

In clinical settings, there are various ways to measure bradykinesia. Usually, a patient is required to perform finger tapping and hand grasping task according to instructions given by the clinicians.

In finger tapping task a subject has to tap index finger with thumb as fast as possible. At the same time amplitude of tapping should be as high as possible. This repetitive task can make patients show different signs essential of bradykinesia if the patient is suffering from the symptoms [22]. Hand grasping task consists of opening and closing of hand [23]. Like finger tapping task, usually patients have to open and close hand with maximum speed and amplitude.

1.2.3 Gait

One of the most severe challenges in dealing with the advancement of PD is an increase in gait instabilities. Gait disturbances include freezing of gait, difficulty in gait initiation, hesitation and shuffling and slow steps [24][25]. Continuous gait disorders affect the step-to-step spatiotemporal dynamics of gait, resulting in increased spatiotemporal gait variability (GV) [26]. The most prevalent outcome measures of GV are second-moment statistics (i.e., standard deviation or coefficient of variation) of a series of step or stride durations or lengths. Generally, during normal walking, the heel strikes the ground before the toes. However, in PD gait, patients walk with flat foot motion (the entire foot is placed on the ground at the same time). Sometimes toe touches before heel for PD patients with advanced stage of the disease. Also, PD patients have reduced foot lifting during the swing phase of gait, which produces a smaller clearance between the toes and the field.

Figure 3. Gait disorder symptoms in PD patients [27]

1.3 Inertial Measurement Unit

An inertial measurement unit (IMU) is an electro-mechanical device that measures an object's acceleration, angular rate, and sometimes the magnetic field surrounding the object. IMU usually has a combination of accelerometers, gyroscopes, and magnetometer to measure these values.

IMU has various applications in many fields. In Inertial Navigation Systems (INS) Angular velocity, attitude, acceleration is often calculated by IMU which is integrated into the system [28]. This INS is the most vital unit of many commercial and military vehicles and navigation such as manned or unmanned aircraft, advanced missiles, ships, submarines, and satellites [29]. They are also essential components in the guidance and control of unmanned systems such as Unmanned Aerial Vehicle (UAVs), Unmanned Ground Vehicle (UGVs), and Unmanned Underwater Vehicle (UUV) [29]. In latest vehicles, an IMU is usually integrated into the navigation system which is

GPS based. By collecting data related to vehicle's speed, acceleration, heading, inclination IMU helps to build today's modern vehicle.

Besides its use for the navigational system, IMUs also has use case as orientation sensors in many vital products. IMUs as orientation sensors are integrated into most of the smartphones and tablet. Fitness trackers and other wearables may also include IMUs to measure motion [29].

IMUs used in the navigational system usually suffer from accumulation error [30] which is its major disadvantage. Because the navigational system is continually integrating acceleration with respect to time for measurement of velocity and position, any calculation errors, however small, are accumulated over time. This leads to a sensor error called drift.
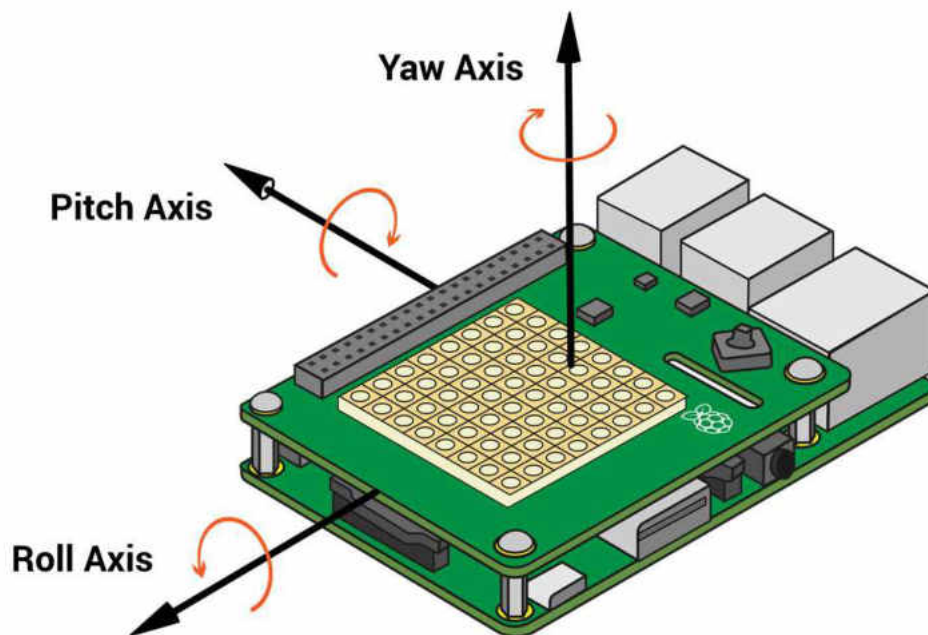
Figure 4. Example of inertial measurement unit. [31]

1.3.1 *Accelerometer*

An accelerometer is an electromechanical device. It mainly measures static and dynamic acceleration forces. An example of static force is gravity pulling at feet. It also measures dynamic forces which are caused by moving the accelerometer [32]. An accelerometer can be built in different ways. Some accelerometers use the mechanism of piezoelectric effect. When a microscopic crystal structure gets stressed by accelerative forces, a voltage is generated. It is called piezoelectric effect [33]. Accelerometer contains this crystal structure to produce this effect. Another way to do it is by sensing changes in capacitance [33]. An accelerometer may contain two microstructures adjacent to each other to sense the change of capacitance [34].

1.3.2 *Gyroscope*

Nowadays gyroscopes are widely used in IMU due to its high performance and reduced footprint. Micro-electro-mechanical systems (MEMS) gyroscopes are also becoming very proficient in power consumption. Because of low production cost, gyroscopes are being integrated into consumer electronics. MEMS gyroscopes measure the angular velocity of an object using Coriolis Effect mechanism. If angular rotation velocity Ω is applied to mass (m) moving in direction v, a force is experienced by the object in the direction of the arrow because of the Coriolis force [35]. Capacitive sensing structure in Gyroscope can sense the resulting displacement caused by the effect of Coriolis force [35].

1.4 MDS-UPDRS Parkinson disease rating scale

Popular rating scale for Parkinson symptoms UPDRS was established during 1980s. Movement Disorder Society (MDS) revised the criteria of original UPDRS rating scale and thus a

new version MDS-UPDRS emerged. MDS-UPDRS scoring rules for three cardinal symptoms of PD [78].

1.4.1 Tremor

Table 1 illustrates the scoring criteria for different severities of tremor [36]

able 1. Tremor scoring criteria for different severity of symptoms according to MDS-UPDRS rating scale [36].

Score	Severity	Symptoms
0	Normal	No shaking of any limbs
1	Slight	Occurrence of tremor but not create difficulty with any activities
2	Mild	Occurrence of tremor causes problems with a few activities
3	Moderate	Shaking or tremor create difficulty with many daily activities
4	Severe	Tremor causes difficulty with all activities

1.4.2 Bradykinesia:

The following table illustrates the scoring criteria for different severities of bradykinesia [36]

Table 2. Bradykinesia scoring criteria for different severity of symptoms according to MDS-UPDRS rating scale [36]

Score	Severity	Symptoms
0	Normal	No problems during finger tapping or hand grasping
1	Slight	One or two hesitation or slight slowing

2	Mild	3 to 5 interruptions or mild slowing
3	Moderate	More than 5 interruptions or moderate slowing
4	Severe	Cannot perform the task because of slowing

1.4.3 Gait

The following table illustrates the scoring criteria for different severities of bradykinesia [36]

Table 3. Gait scoring criteria for different severity of symptoms according to MDS-UPDRS rating scale [36]

Score	Severity	Symptoms
0	Normal	No difficulty during walking
1	Slight	Can walk independently with minor gait impairment.
2	Mild	Can walk independently with substantial gait impairment
3	Moderate	Require assistance for walking
4	Severe	Cannot walk

1.5 Current Practice and Quantification Methods in PD Symptoms

1.5.1 Tremor

Currently, PD tremor is usually assessed in clinical settings where a patient has to complete predefined motor tasks. A physician assigns a score based on the Unified Parkinson's Disease Rating Scale (UPDRS) after observing the motor task [36]. However, this procedure suffers from intersubject variability. Also, patients tend to show fewer symptoms during clinical visits

potentially skewing assessment of their disease severity [37][38]. A study conducted by Giuliano on interobserver reproducibility of the score for most frequently used PD rating scale. The experiment involved 48 patients. Their study concluded that the clinician's score for PD symptoms varied substantially among them.

To overcome this limitation, various attempts to quantify PD tremor have been made. These include the use of electromyography (EMG) [39], electromagnetic tracking [40] and laser-based displacement transducer, and infrared cameras for objective assessment of tremors [41]. In Bacher's study [15], PD and essential tremors were recorded continuously using surface EMG recording from forearm. Electromagnetic tracking system for tremor quantification [16] was validated with a sample of 23 patients. The accuracy of the device and algorithm was confirmed by mechanically generating oscillations of known magnitudes and frequencies. Although these approaches do quantify tremor, they are often of large dimension and bulky making them uncomfortable for patients to use.

Recently, the use of micro-electro-mechanical system (MEMS) inertial measurement units has been deployed for assessment of tremor in several studies. Nizmant et al. quantitatively assessed tremor using a sensor system integrated into a smart glove [42]. The glove had two touch sensors, two 3D accelerometer and one force sensor to measure primary motor symptoms tremor and bradykinesia. Although they claim the prototype is easy to wear, tremor and bradykinesia assessment algorithm needs to be expanded to consider more parameters. Only tremor frequency and movement time between finger tapping were the parameters considered for tremor and bradykinesia symptoms evaluation using their prototype. Salarian et al. placed a three-dimensional gyroscope on the wrist for continuous monitoring of tremor [12]. This was one of the first studies which established the use of inertial measurement unit to quantify PD symptoms. Here, the sensors

was placed on each of the forearms. An algorithm to detect and quantify tremor and another algorithm to quantify bradykinesia have been proposed and validated. In addition, Salarian et al. presented a continuous tremor symptoms monitoring system with 3D gyroscope placed on the wrist position [4]. The Motus Movement Monitor (Motus Bioengineering Inc., Benicia, CA, USA), was used to quantify tremor and other symptoms [43]. The system was based on three axis gyroscopes. They also assessed dyskinesia using their rotation sensitive movement monitor and evaluate the asymmetry of the dyskinesia between the right and left side. Pierleoni et al. used combination of an accelerometer and a gyroscope on wrist, to determine type and severities of tremors [44]. Their study can detect types of tremor (resting, postural, kinetic) and correlation with UPDRS score stated to be satisfactory.

Khan et al. developed a wearable senssor system based on accelerometer to predict and classify tremors based on several machine learning algorithms, especially the non-linear radial basis function kernel [32]. In their study, they first developed the program of a detection system to distinguish between normal and Parkinsonian signal in the accelerometer data, as well as to classify different types of PD symptoms. The system was then evaluated in 12 patients suffering from PD. Zhang et al. developed an accelerometer sensing system to assess tremor signal in real time during daily life activities. The method combines the time and frequency domain analysis of signals. The frequency domain analysis is performed using short-time Fourier transform to reduce the instability of the tremor signals [45]. Furthermore, the combination of an accelerometer and a gyroscope in a wrist module was used to objectively measure and classify tremor in another study in order to achieve more effective results [44]. Most recent study for automatic tremor scoring system using Inertial measurement unit was done by Jeon et al. [46] Here Parkinson tremor was assessed for 84 subjects using fingers placed on sensor and 85.5% prediction accuracy was

achieved using Decision tree algorithm. Following this strategy of assessment of tremor, placement of the sensors is also an important factor in determining the accuracy of the system. Currently, the finger and wrist have been examined as sensitive locations to quantify tremor in several studies [44]. However, whether placing sensors on the finger and wrist at the same time leads to better identification and classification of tremor needs to be explored further.

Feature extraction from sensor data is another important aspect of tremor quantification and severity classification. Giuffrida's research showed that the logarithm of the summation of accelerometer and gyroscope peak power around the dominant frequency correlates well with UPDRS ratings [47]. This study also presented that the logarithm of RMS summation of angular velocity and linear acceleration signals along all axes linked best with the UPDRS scores. However standard deviation of angular velocity and linear acceleration is an important parameter that is missing from their analysis.

1.5.2 Bradykinesia

The current method of assessing bradykinesia requires patients to perform certain motor tasks in clinical settings [46]. An UPDRS score is assigned to each task based on the observation by a physician. However, patients do not always show natural PD symptoms during a clinical visit. Also, subjective bias occurs during such assessment of bradykinesia. To overcome these limitations, several attempts have been made to quantify bradykinesia using wearable sensors [48]. Accelerometer, gyroscope or a combination of both have been employed for acquisition of movement data to evaluate bradykinesia [48].

Salarian et al. presented a gyroscope-based continuous monitoring system for objective assessment of wrist bradykinesia [11]. The system reported in the study was easy to use and record movement signal from wrist. The study recorded signals continuously for up to 14 hours during

daily activities of patients. Range, periods of movement and amplitude parameters correlated well with the UPDRS scores of bradykinesia (r = −0.73 to −0.83, p = 0.001) [12].

Kim et al. quantified bradykinesia during finger taps by using a gyroscope [48]. Forty PD patients and 14 age-matched control subjects participated in the experiments conducted by Kim et al. [48]. Subjects' finger taps in both right and left hands were scored by two independent neurologists according to the unified PD rating scale and were also measured by a gyrosensor. Among the analyzed features, RMS (root-mean-square) velocity, RMS angle, and the average power around the dominant frequency correlated well with clinical UPDRS scores of finger tapping (r = −0.73 to −0.80, p = 0.001) [49].

Heldman et al. presented a wearable sensor system to assess lower extremity bradykinesia [49]. The Kinesia Home View system developed by Heldman et al. which include a touch-screen tablet computer, a finger worn motion sensor unit and docking station was attached to heel-clip for lower extremity bradykinesia evaluation [50]. Heldman et al. also developed a hand bradykinesia assessment system, whose correlation coefficient is 0.67 with modified bradykinesia rating scale. Fifty patients with PD performed UPDRS–directed finger tapping, hand grasping, and pronation–supination while wearing motion sensors [51].

Printy et al. developed a smart phone application for quantifying bradykinesia of finger (r = −0.48, p = 0.04) [52]. Modern smart phones have IMU integrated into it thus having the capability to serve as widely available medical diagnostic devices. By keeping this thing in mind, their study developed an iPhone application that recorded data from small sample of PD patients during guided bradykinesia assessment task. [52]. Dunnewold et al. tested subjects with PD disease for objective evaluation of Parkinson bradykinesia. A total of 33 patients with Parkinson's disease and 29 healthy controls performed a predefined task consisting of a tap rate test and movement time

test [53]. Accelerometers were placed on wrist to capture movement signal during wrist taping. They concluded as mean acceleration of movement as reliable parameter to evaluate bradykinesia [53]. Zwartjes et al. designed an accelerometer-based ambulatory monitoring system to classify symptoms severity [54]. Their algorithm provided a detailed assessment of tremor and bradykinesia symptoms. Besides evaluation of symptom severity, their system could also differentiate between different activity done by patients [54].

Most recent works on bradykinesia quantification has been done by Martinez et al. [48]. In his study, a system for objective assessment of bradykinesia was developed to eliminate ambiguity of an evaluator as different evaluators might score movement features differently. Therefore, the features selection procedure was performed using the scores of four clinical evaluators, separately. Support Vector Machine (SVM) classifier was finally used to classify symptoms of different severity using selected features.

Time-domain parameters derived from sensor signals for characterizing bradykinesia which includes speed, amplitude, hesitations, and halt have been evaluated in previous studies [48][12]. However, the effect of frequency domain parameters and non-linear features extracted from sensor signals for evaluating the severity of bradykinesia is unknown. Whether or not it leads to an improvement in the assessment of bradykinesia needs to be investigated. It is known that the patients suffering from severe bradykinesia have their movement signal distorted due to unpredictable movement or hesitation [55]. Nonlinear features can characterize the degree of complexity and provide further relevant insights regarding the severity of bradykinesia..

1.5.3 Gait

Analyzing gait parameter has been widely studied for both healthy and disease populations [56]. Gait speed is the most common gait characteristic that is widely used to diagnose disease or

monitor progress of gait rehabilitation [57]. In spite of various implementation of gait measurement system, there is always rooms for improvement to make the system more comfortable and efficient to measure gait parameter and assist clinicians in decision making. There are a number of gait analysis systems currently in use to measure gait. The more traditional approach in clinical setting is to use a stopwatch to measure time to finish a predefined walking through a known distance. Optical motion capture technology is industry standard for analysis of gait [58]. Although it is very accurate in measurement, the cost and size of the machine make it unsuitable for environment outside laboratory settings. That's why ambulatory gait monitoring system has been of much interest lately [59].

Different wearable sensors have been used in literature for ambulatory estimation of gait speed [59]. Pressure insoles integrated into shoes have been used to accurately detect the different phase of gait which is key to extract different characteristics of gait such as stride length and gait speed[59][60]. To obtain more information from gait, the use of accelerometer and gyroscope has been gradually increased in last decade[61][62][63][40]. Increasing efficiency and low cost of miniature inertial sensors are also helping to make it an easy choice for gait speed measurement experiment. The spatio-temporal parameters measured by inertial measurement unit (IMU) reported in these studies include walking speed, stride length, and total walked distance.

There is a repeated cyclic movement of body segments during walking in every stride cycle. Inertial sensor attached to body can analyze the movement and measure change of acceleration and angular velocity during walking. Based on application, inertial sensor can be placed at different parts of the body. Different methods of obtaining gait speed have been proposed by many researchers lately. Aminian et al. developed a walking speed estimation algorithm from accelerometer signal as inputs where artificial Neural network (ANN) with four input layers and

two hidden layers was used for data processing [64]. However, the accuracy of the estimation was very low due to use of abstraction model instead of actual physical system. Human gait model has also been adopted by some researchers to estimate parameters like gait velocity, stride length and total walking distance. Simplified gait model based on human walking motion and biomechanics had been applied in several studies to reduce sensor configuration and computational complexity. Miyazaki proposed a symmetric gait model to calculate stride length and walking speed estimation method using a gyroscope attached to the thigh [65]. Tong et al. also did a significant work in using human gait model for estimation of gait speed where he modeled each leg as an individual segment and shank attached gyroscope was used for data collection [66]. The relative error achieved by both of the studies were 15% which is not acceptable for clinical diagnosis and rehabilitation applications.

In recent years, the use of direct integration technique to estimate walking speed has become more popular. To the best of our knowledge, the first direct integration method used for walking speed approximation was proposed by Sabatini et al. in 2005, which used an IMU (biaxial accelerometer and biaxial gyroscope) placed on the instep of the foot [67]. The average error rate of their proposed system was 0.18 km/h. Alvarez extended Sabatini's analysis and presented a technique to combine the information gained from multiple sensors that potentially improved the walking speed approximation accuracy [68]. However, the distance covered by subjects during those measurements is 10 m only. The algorithm performance for relatively long distance is unknown.

PD patients tend to have specific walking pattern in comparison to normal subjects. Variability from stride to stride can be seen in a patient from early stage to advanced stage of PD. The magnitude of variations can be directly correlated to disease severity. Among different PD

symptoms, gait variability is closely linked to risk of falls on elderly PD patients. Inability to sustain steady gait with greater gait cycle to cycle variations also is dependent on gait speed and healthy aging effects [69]. Gait variability of PD with link to disease severity and falls are investigated in several studies [70][71][72]. PD patients also considered to have contact with floor more than normal subjects. This characteristic leads to more average stance time and less average swing time compared to normal patients. Swing and stance phase of PD patients with respect to disease severity have been investigated by Shyam et al. [73]. Generally, during normal walking, the heel strikes the ground before the toes. However, in PD gait, patients walk with flat foot motion (the entire foot is placed on the ground at the same time). Sometimes toe touches before heel for PD patients with advanced stage of the disease [74]. Luca et al. conducted a study to find gait pattern before Freezing of Gait episode using Inertial Measurement unit. [75]

In addition, PD patients usually can't lift foot like normal people during the swing phase of gait thus producing smaller clearance between the toes and the surface [76]. During heel strike, patients with PD have reduced impact. Intensity of the impact keeps decreasing with the progression of the disease [77].

.

CHAPTER 2

PROPOSED METHODS

In this chapter, we would first discuss the protocol, demographic of the subjects recruited. Then proposed methodology to process sensor signal, extract and analyze parameters would be described. Last part of the chapter includes a brief introduction to different classifier we used.

2.1   Data Acquisition

2.1.1   Subjects

To develop preliminary algorithm and test the feasibility of the system, data was acquired from 14 subjects who did not have PD or any neurodegenerative disorder but were educated about PD symptoms (tremor, bradykinesia, gait) and shown how to emulate it appropriately. Subject testing was approved by University of North Dakota IRB, and each subject signed a consent form. Each subject emulated rest and postural tremor for 25 to 30 seconds for low, medium, and high intensities. These intensities were intended to mimic UPDRS scores 1, 2, and 3, respectively. For resting tremor, subjects had to sit still and place their hand in their lap. To mimic postural tremor, subjects had to extend their hand in front of their body. The Physilog Gold wireless inertial measurement unit made by Gait Up was used to collect data. For bradykinesia measurement, eight subjects who did not have PD or neurodegenerative disorders were trained by an expert physician to emulate bradykinesia for different UPDRS scores. They were asked to tap interphalangeal joint of thumb using their index finger. Each subject did four trials to mimic UPDRS scores of 0, 1, 2 and 3 and their performance were scored by a physician trained in UPDRS assessment. Subjects were instructed to stop after completing 10 finger tapping task. For gait speed measurement, Total

5 subjects participated in the trial of treadmill walking. All the participants were healthy and did not have any motor or neurological disorder. Each subject was instructed to walk on a treadmill for one minute for four different selected speeds: 0.5, 1, 2 and 3 miles/hour.

Nineteen Patients with PD participated in the study using the Physilog Gold wireless inertial measurement unit to assess tremor, bradykinesia and gait. The Sanford Health IRB approved the study. Subject 1 was excluded from the study because the UPDRS scores were not obtained. Subject 17 was excluded because the patient took medicine the morning of the study visit.. Table 4 includes the demographics of the subjects recruited for the experiment whereas Table 5 listed the medication information and doses used by the patients. The UPDRS scores while off and on PD medications are listed in the Table 6 and Table 7 respectively. Details about the data collection process is described in the protocol section.

Table 4. Demographics of subjects attended in the clinical trial.

Subject#	Date	Gender	Age	MOCA	Date of MOCA	UPDRS Pre	UPDRS Post

1	4/14/2017	M	73	25	11/10/2016	n/a	n/a
2	4/28/2017	F	61	28	4/28/2017	3	0
3	5/5/2017	F	59	28	2/28/2017	15	8
4	5/5/2017	M	81	24	5/5/2017	22	11
5	5/12/2017	F	79	28	10/28/2016	12	6
6	5/12/2017	F	65	27	12/19/2016	25	14
7	5/19/2017	F	65	27	2/10/2017	5	5
8	5/25/2017	M	64	25	12/13/2016	33	28
9	5/26/2017	M	69	29	2/24/2017	11	13
10	6/2/2017	M	82	24	6/2/2017	2	22
11	6/8/2017	M	61	28	2/27/2017	3	37
12	6/16/2017	F	64	25	6/16/2017	1	33
13	6/26/2017	F	57	28	4/10/2017	3	47
14	7/6/2017	M	75	28	7/6/2017	2	42
15	7/20/2017	F	68	28	5/23/2017	2	32
16	7/21/2017	F	67	26	7/21/2017	1	6
18	7/28/2017	M	64	27	6/30/2017	1	14
19	8/18/2017	M	65	26	8/18/2017	2	31

Table 5. Medication information of Parkinson patients

Subject No	Date	Age	DBS	Medication	Class	Times/Day	Dosage	LEDD (mg)
1	4/14/2017	73	No					
2	4/28/2017	61	No	Sinemet	Carb/Levo	2 tablets 4x/day, 1 at bedtime and 1 middle of night	25-100	1000
3	5/5/2017	59	No	Sinemet	Carb/Levo	2 tablets 6x/day	25-100	1200
4	5/5/2017	81	No	Sinemet	Carb/Levo	1.5 tablets 3x/day	25-100	450
5	5/12/2017	79	No	Sinemet	Carb/Levo	1.5 tablets 4x/day	25-100	600
6	5/12/2017	65	No	Sinemet	Carb/Levo	1 tablet 4x/day	25-100	400
7	5/19/2017	65	No	Azilect	MAO-B Inhibitor	1/day	1	100
8	5/25/2017	64	Yes	Sinemet	Carb/Levo	1 tablets 5x/day. add'l .5 if needed	25-100	650
9	5/26/2017	69	No	Sinemet	Carb/Levo	2.5 tablets 4x/day	25-100	1000
10	6/2/2017	82	No	Sinemet	Carb/Levo	2 tablets 3x/day	25-100	600
11	6/8/2017	61	No	Sinemet	Carb/Levo	2 tablets 3x/day	25-100	600
12	6/16/2017	64	Yes	Rytary	Carb/Levo	1 tablet 5x/day	48.75-195	975
13	6/26/2017	57	Yes	Rytary	Carb/Levo	2 capsules 4x/day	36.25-145	696
14	7/6/2017	75	No	Requip	dopaminergic	3 tablets 3x/day	2	360
15	7/20/2017	68	No	Sinemet	Carb/Levo	1 tablet 3x/day	25-100	300

16	7/21/2017	67	No	Sinemet	Carb/Levo	1 tablet 3x/day	25-100	300
18	7/28/2017	64	No	Sinemet	Carb/Levo	3 tablets 3x/day	25-100	900
19	8/18/2017	65	No	Sinemet	Carb/Levo	1.5 tablets 6x/day	25-100	900

Premedication:

Table 6. Off-medication UPDRS scores for different tasks

Subject#	Date	Side	Rest Tremor	Postural Tremor	Finger Tap	Hand Grasp	Gait	Total
1	4/14/2017				N/A			
2	4/28/2017	L	0	0	0	0	1	1
3	5/5/2017	L	0	0	1	0	2	3
4	5/5/2017	L	1	0	2	2	0	5
5	5/12/2017	L	1	0	1	0	0	2
6	5/12/2017	L	0	0	1	1	2	4
7	5/19/2017	L	0	0	2	0	0	2
8	5/25/2017	R	0	0	1	1	1	3
9	5/26/2017	R	0	0	1	0	1	2
10	6/2/2017	L	0	0	2	0	1	3
11	6/8/2017	R	2	2	1	2	3	10
12	6/16/2017	L	0	0	3	3	2	8
13	6/26/2017	R	0	1	2	1	4	8
14	7/6/2017	L	2	0	3	2	1	8
15	7/20/2017	L	2	1	2	2	1	8

16	7/21/2017	R	0	0	0	0	0	0
18	7/28/2017	L	1	0	2	0	1	4
19	8/18/2017	R	1	1	3	2	0	7

Post-medication:

Table 7. On-medication UPDRS scores for different tasks

Subject#	Date	Side	Rest Tremor	Postural Tremor	Finger Tap	Hand Grasp	Gait	Total
1	4/14/2017				N/A			
2	4/28/2017	L	0	0	0	0	0	0
3	5/5/2017	L	0	0	0	0	0	0
4	5/5/2017	L	0	0	1	0	1	2
5	5/12/2017	L	0	0	0	0	0	0
6	5/12/2017	L	0	0	1	0	1	2
7	5/19/2017	L	0	0	0	0	0	0
8	5/25/2017	R	0	0	1	2	0	3
9	5/26/2017	R	0	1	2	1	0	4
10	6/2/2017	L	0	0	1	0	1	2
11	6/8/2017	R	1	2	1	1	3	8
12	6/16/2017	L	0	0	3	3	2	8
13	6/26/2017	R	0	1	1	1	4	7
14	7/6/2017	L	1	0	2	2	1	6
15	7/20/2017	L	1	0	1	1	0	3
16	7/21/2017	R	0	0	0	0	0	0

18	7/28/2017	L	1	0	1	0	0	2
19	8/18/2017	R	1	1	3	1	0	6

2.1.2 Measurement System

The Physilog®4 is a lightweight (19g) and fully stand-alone wireless inertial measurement unit [79]. Physilog®4 Silver contains 10 MEMS sensors (3D accelerometer + 3D gyroscope + 3D magnetometer + 1 barometric pressure sensor) [79]. Physilog®4 Gold records, in addition, either GPS, ECG data, or other Analogic signals. Sampling frequency is programmable between 50Hz and 1KHz. In this study, sampling frequency was set to 100 Hz. Unlimited number of sensors can be synchronized wirelessly for multi-segment motion capture. Raw data can be extracted and processed with a library of functions provided by Gait Up and/or third-parties [79]. This stand-alone system is comfortable to wear, and provides truly reliable motion data indoor and outdoor.
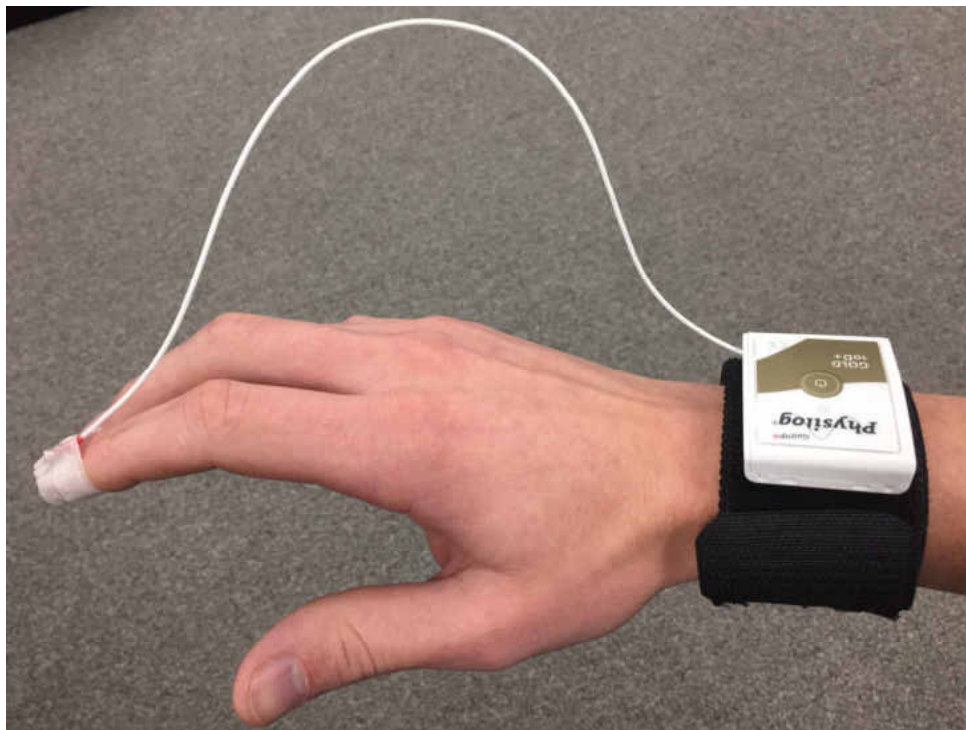
Figure 5. Physilog device attached to the subject for measurement [79]**.**

2.1.3 Protocol

Subjects came to the laboratory before they took the first dose of their PD medications (i.e. the last dose of their medication was the night before). We obtained MDS-UPDRS motor scores. We then used the Physilog Gold Inertial Measurement (PGIM) to assess tremor, bradykinesia, and gait. During the visit, the patient took their first dose of prescribed medication of the day after the initial PGIM assessment. Delaying the dose until the dose during research testing caused minimal clinical risks. The patient might experience more tremor, rigidity, and bradykinesia. These symptoms are common at the end of each dose, even during the days when they were not participating in the study. Exact time intervals between these two doses depended on when a patient takes the last dose of medicine the night before. Typically, a patient takes their last dose for the day at 6-7 pm and takes the first dose of the day when wakes up, usually 6-7 am. Because we scheduled the patient for the testing first thing in the morning (about 8 am), they were able to take their regular medicine no later than 930 am. A second PGIM assessment of tremor, bradykinesia, and gait were taken 45 minutes after taking their medication. 45 minutes would be enough time to wait after taking the PD medication because it takes Sinemet (Carbidopa/Levodopa), the most commonly prescribed meds for PD, 30 minutes to kick in. A PD patient may take one or more of the following medicines: Commonly used:Carbidopa/levodopa (Sinemet); Pramipexole (Mirapex); Ropinolol (Requip); Less commonly used: Amantidine (Symmetrel); Selegiline (Eldepryl); Rasagiline (Azilect); trihexyphenidyl (Artane).

1. Tremor. For tremor analysis, we have placed the sensors at the distal end of the third metatarsal bone, the extensor surface of the forearm 10 cm proximal to the wrist, and extensor surface of the upper arm 10 cm to the elbow of the more affected hand. The hand was splinted to

prevent movement of the metacarpal joints, proximal interphalangeal joints, and distal interphalangeal joints of the second, third, fourth, and fifth fingers. Tremor activity was measured with the arm and the hand resting on the thigh for 30 seconds to measure rest tremor and with the arm outstretched in a horizontal position for 30 seconds to measure posture tremor.

2. Bradykinesia. For bradykinesia analysis, a sensor was placed at the dorsum of the tip of the index finger of the more affected hand. The subject used the index finger to tap the interphalangeal joint of the thumb as fast as possible for 30 seconds. In a separate trial, they opened and closed their palm as fast as possible for 30 seconds.

3. Gait analysis. For gait analysis, sensors were attached to the heel cap and the toe cap of the shoe on the more affected side. Another sensor was placed at the wrist to measure the amplitudes of arm swing. The subjects walked as fast as possible for 10 meters, turned around, and walked back to the starting point. A research personnel walked with the patients and catch the patients in case they lose their balance.

Data were then transferred from the sensors to Laptop. The signal processing program developed in our laboratory analyzed the data collected and generated the primary outcome measures listed above.

2.2 Tremor Signal Processing

We first developed algorithm for mock patients who were instructed to emulate the resting and postural tremor for different severities. Next, the algorithm were tuned when the algorithm was tested with patients before and after medication.

In the algorithm developed to analyze mock patients data, the preprocessing and tremor detection process (used to validate appropriate emulation of tremor) used was similar to that used in the study done by Salarian *et al.* [12]. The notable differences in the process used for this study are the inclusion of the accelerometer signals, multiple locations (wrist and finger), no dominant frequency amplitude threshold used for the detection process, and the use of Welch's method of spectrum analysis. For the preprocessing and tremor detection, MATLAB software as used, and each axis was analyzed separately. In the first step, the drift present in the signals was removed using a high pass Butterworth infinite impulse response (IIR) filter with a cutoff frequency of 0.25Hz. Next, the signal was divided into 3-second windows in order to optimize tremor detection. For each window, the frequency spectrum of the signal was calculated using Welch's method. Next, the pole with the highest amplitude was considered the dominant pole. If its frequency was between 3.5 and 7.5 Hz (PD tremor range) [42][80], the window was classified as a tremor window.

After this preprocessing and tremor detection, the results for each trial were analyzed to determine if the emulated tremor was confirmed to be adequate. This was done by using a tremor detection threshold of 80%. Therefore, of the six windows from each signal, over 80% had to have a dominant frequency in the PD range in any of the three axes of both the accelerometer and gyroscope. If this was the case, the entire 20-second window was considered PD tremor and it was used for quantification analysis. The power spectral density of subject 1 is shown in Figure 3 as a reference of adequately emulated tremor. Using this process, two sets of resting tremor trials and three sets of postural tremor trials were excluded.

One noticeable difference we used is determination of dominant axis using principal component to determine dominant axis of tremor. Overall system to predict tremor score is shown in the Figure 7.

Detrending method was used to detrend the signal using Matlab detrend command. The MATLAB® function detrend subtracts the mean or a best-fit line (in the least-squares sense) from the data [81]. Removing a trend from the data enables to focus our analysis on meaningful fluctuations in the data. A linear trend points to increase or decrease in the information systematically [81]. In case of Inertial Measurement Unit, a systematic shift results from sensor drift. For example, a IMU signal before and after detrending is shown in Figure 8. From the figure it is seen that signal after detrending operation centered around 0 value which was not the case before detrending operation because of sensor drift. While trends can be meaningful, here analyses yield better insight once you remove trends [81].

Median filter was used to smooth the signal by suppressing noise. The median filter works by running through the signal value by value, replacing each value with the median of neighboring entry values [82]. The median filter window slides over the entire signal and filters each element of the signal. Butterworth filtering was used in the same way it was used for first experiment. However, instead of 3 second window 10 second window was used to analyze the tremor signal more efficiently. 10-second window gives 1000 sample where we can run welch's algorithm to compute Power Spectral Density. If the input signal is x, the function used for PSD calculation returns PSD estimate, pxx. Welch's overlapped window averaging estimator was used to compute pxx. x is considered a single channel when it is a vector. For x as a matrix, each column is considered a channel and the PSD is computed for each column of input signal matrix and stored in the corresponding column of PSD signal. If x is real-valued, output pxx is a one-sided estimate

of power spectral density. If x is complex-valued, output pxx is a two-sided estimate of power spectral density. According to welch's algorithm to obtain PSD, x is divided into the 50% overlapping segments. Segments were chosen such that total no of segments gets close to but not exceed 8. Hamming window is used for each segment. The average of modified period-grams are taken to obtain the PSD estimate. So in case, input vector x can not exactly get divided into an integer number, x would be truncated accordingly. The function also returns f as a frequency vector, f (cycles/unit time). The sampling frequency, fs, can also be given as an input parameter to the function. The number of samples per unit time is called sampling frequency [83].

Flowchart for signal processing algorithm is shown below in Figure 6
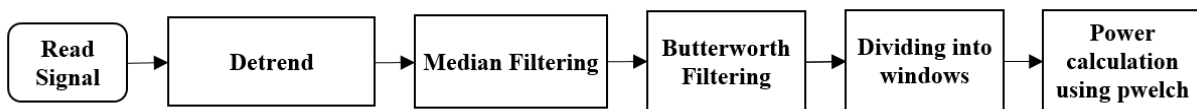
Figure 6. Flowchart for signal processing algorithm
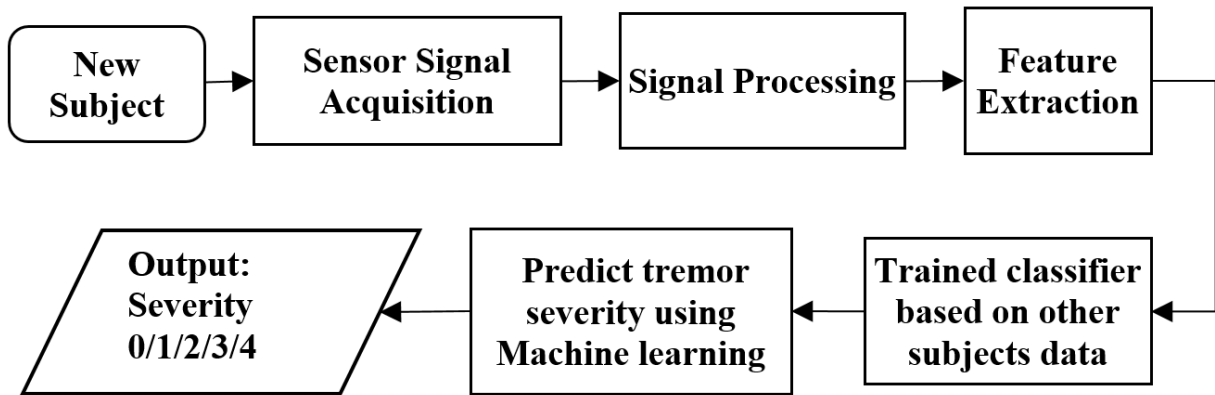
Figure 7. Flowchart for operation
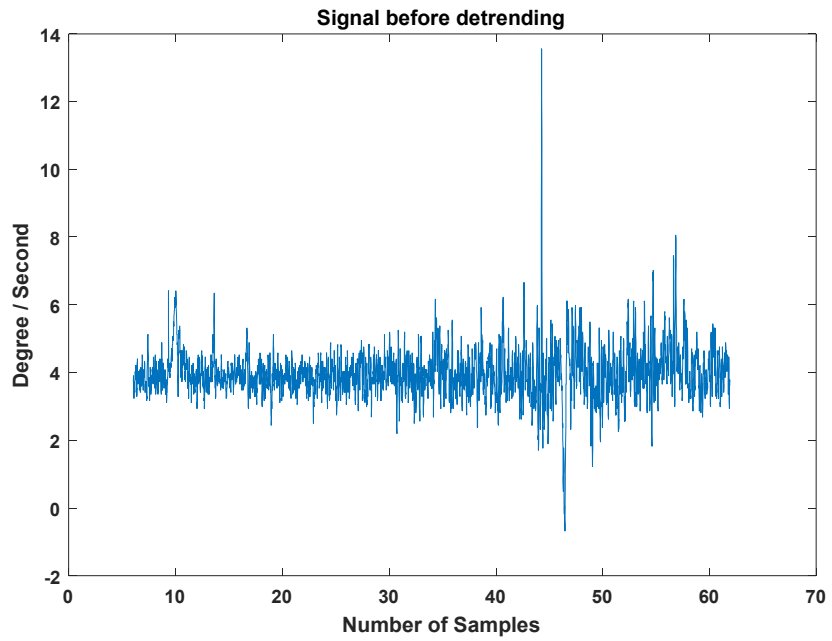
(a)
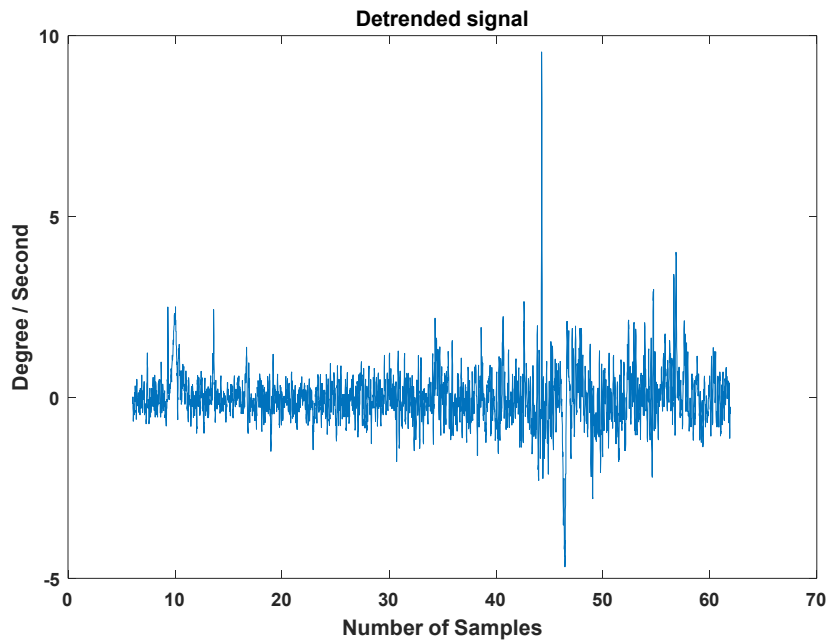
(b)

Figure 8. Detrended signal (a) before the detrend operation and (b) after the detrend operation. The signal centered around 0 after detrending operation.
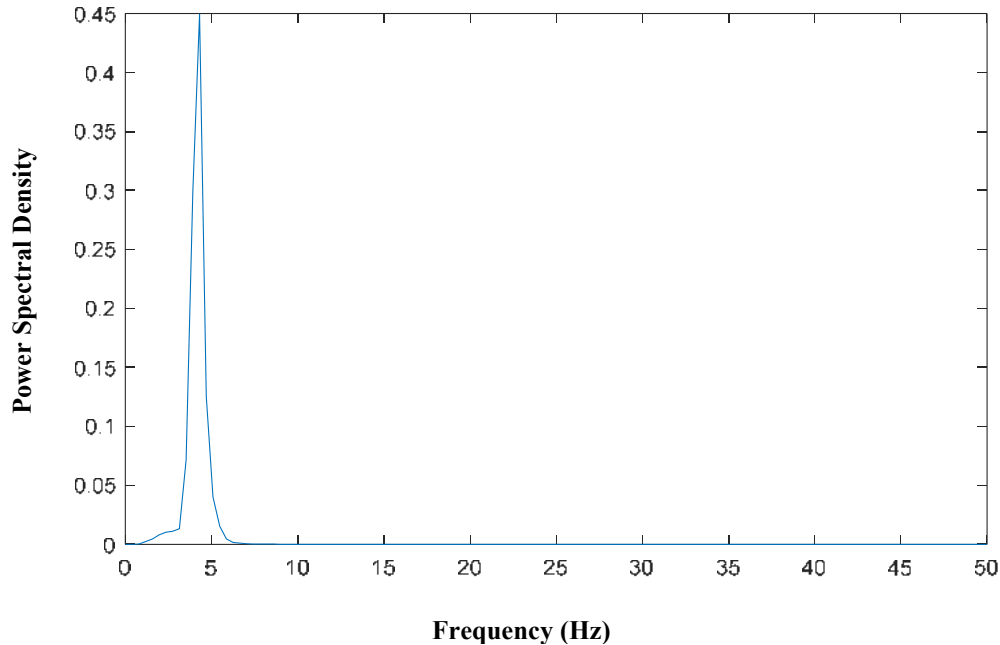
Figure 9. Power calculation using Pwelch. The PSD curve has a peak around 5 Hz.

2.3 Gait Analysis

For Gait analysis Software provided by GaitUp was used to collect spatio-temporal parameters from Inertial measurement Unit [84]. All the parameters obtained before and after medication would be discussed later. We first experimented with healthy patients data to come for an algorithm for speed measurement. Total 5 subjects participated in the trial of treadmill walking. All the participants were healthy and did not have any motor or neurological disorder. Each subject was instructed to walk on a treadmill for one minute for four different selected speeds: 0.5, 1, 2 and 3 miles/hour. As the speed would be measured on real world coordinate, acceleration in sensor axis is converted to real world axis form orientation information extracted from gyroscope signal. Foot acceleration can be projected from sensor acceleration using following equations:

$$A_x = a_x \cos(\theta) - a_z \sin(\theta) \dots\dots\dots\dots\dots\dots\dots\dots(1)$$

$$A_z = a_x \sin(\theta) - a_z \cos(\theta) - g \dots\dots\dots\dots\dots\dots(2)$$

34

where A_x and A_z foot acceleration in X and Z axis and a_x and a_z are sensor outputs. θ is angle computed by integration of gyroscope signal around Y axis. After this step, gait cycle was divided in four different phases by analyzing peaks of angular velocity signals obtained from gyroscope (Figure 10). Four detected points were: stance, heel-off, swing and heel-strike (HS). The segmentation procedure was developed in MATLAB following the works done by Sabatini [67]. As treadmill speed is aligned with x direction of foot sensor, velocity in x direction is considered as gait speed. To accomplish that, strap-down integration of foot acceleration was done using the following equations on foot moving period of a gait cycle:

$$v_x = INT \left[\int_{T_{start}}^{t} a_X(\tau)d\tau \right] \ldots\ldots\ldots\ldots\ldots\ldots\ldots\ldots\ldots(3)$$

where v_x is velocity in x direction, $Tstart$ is the point of beginning of toe off and t is end of heel strike. As human gait is cyclical, integration is started when foot started moving from foot flat position in each gait cycle and integration stops at the beginning of next foot flat period. A zero-velocity update method was applied to estimate initial velocity before each gait cycle.
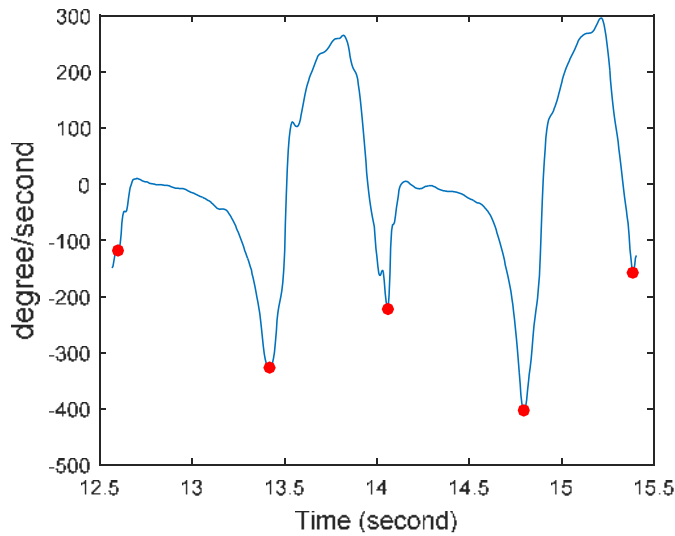
Figure 10. Detection of peaks in angular velocity signal for gait phase segmentation.

35

2.3.1 Kalman filter

Kalman filtering (KF) was used to reduce the noise of a signal by removing uncertainty [85]. The velocity calculation by integrating the acceleration signal tends to produce noisy results. To fix this, KF can be used to fine tune the estimated velocity and improve the result. KF is also used for predicting the future states. In our study, a KF was implemented to estimate current velocity by reducing the effect of integration error. The estimation process through KF mainly works based on prediction equation and update equation. The prediction equation estimates the current state based on the previous state of the system while update equation is used to check the prediction accuracy.

2.4   Bradykinesia

For our setup, during finger-tapping and hand-grasping task albeit, the angular velocity is dominant along y-axis. But due to the existence of movement in other axes and also to reduce axis bias of sensors, angular velocity data from other axes were also considered. Any drift that might have gotten incorporated due to sensor noise was filtered by using a band pass filtering with a bandwidth of 0.3 Hz-20 Hz. Next, we developed an automatic segmentation algorithm to segment each cycle of finger tapping or hand grasping angular velocity signal based on frequency of taping or grasping. The average time for each finger tapping was calculated. Then the width of the minimum peak distance to detect peak in angular velocity signal was set as 0.7 multiplied by the width of the tapping interval. The minimum height of peak was set as 0.20 multiplied by the length of highest peak. These thresholds were selected based on trial and error basis on available datasets. If a patients have severe PD, these values may have to be adjusted. Findpeaks function of

MATLAB was then applied to detect peaks that indicate completion of each cycle of a task (finger tapping or hand grasping).
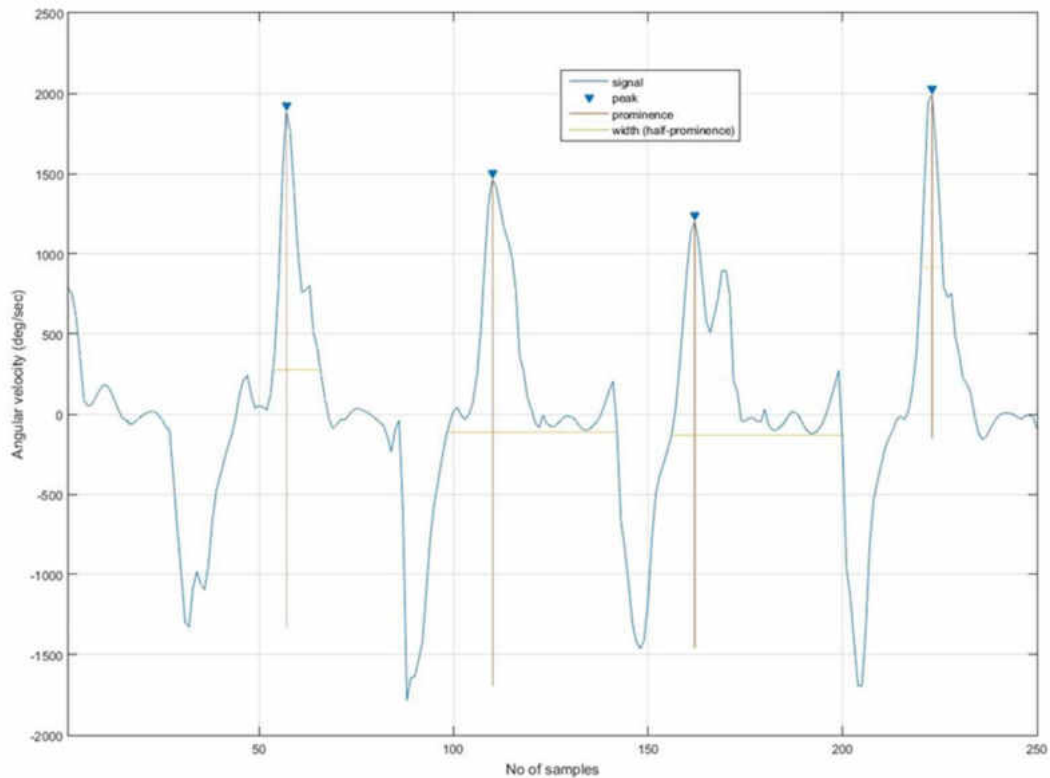
Figure 11. Before medication finger tapping. Peaks are detected using automatic peak detection algorithm. 2.5 seconds of data with a sampling frequency of 100 Hz is shown in the figure

After signal processing stage, signals were passed into the feature extraction algorithm. As we distinguished each finger or hand palm closing points using peak detection techniques, we segmented the interval between each peaks to a separate matrix. After that the maximum value of each segment signal was calculated which indicates the maximum opening velocity of finger or hand palm. We also calculated the mean and standard deviation of each tapping interval and took

it as a feature. Hesitations was quantified when tap time was well below and above mean tap time of the signal.
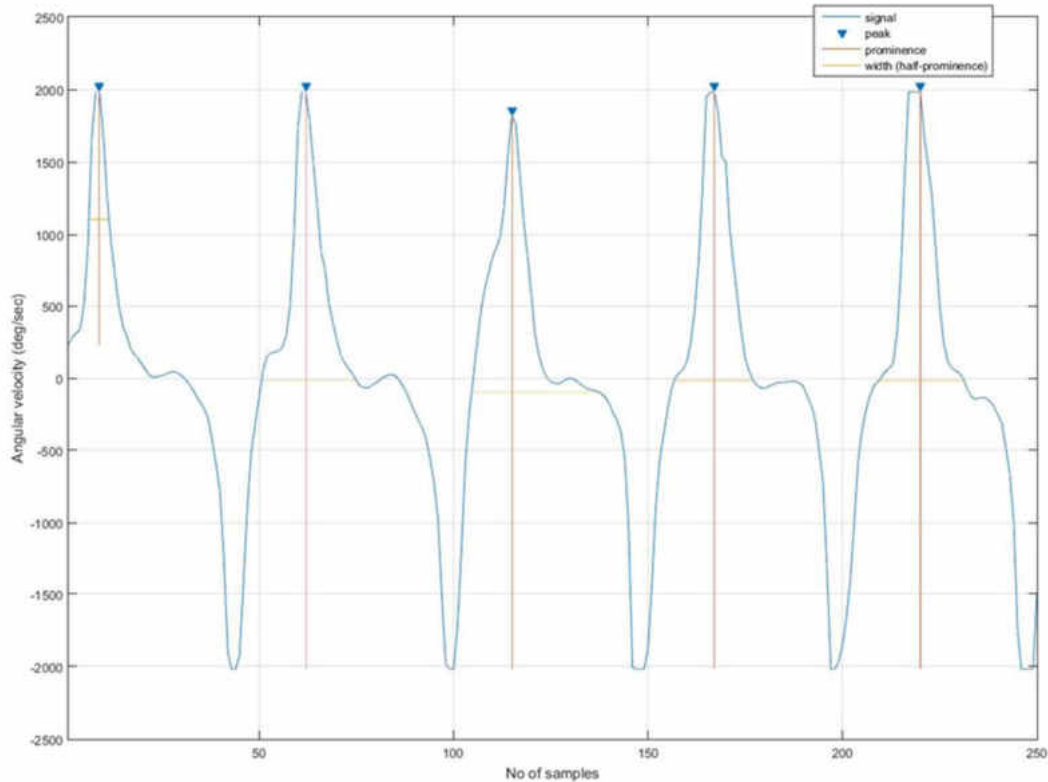
Figure 12. After medication finger tapping. Peaks are detected using automatic peak detection algorithm. 2.5 seconds of data with a sampling frequency of 100 Hz is shown in the figure

2.4.1 Classification

The accuracy of a classification technique is judged based on prediction accuracy. There are three common techniques to evaluate the prediction accuracy. First technique is to split a certain portion (generally two third) of whole dataset to use as training set to train the classifier while using the rest data as test set to evaluate the prediction performance. Another technique is known as cross

38

validation where the dataset is divided into equal sized mutually exclusive subsets and for one subset, classifier is trained by the union of other subsets. The average of error rate is than used as the error rate of the classifier. The third technique is leave one out method which is mainly used for small dataset. This is a special form of cross validation where only one instance is used as test set while all other data are used for training the classifier. This is the most computationally expensive method but useful for a more accurate estimation of classifier performance. For our system, we used five-fold cross validation method to predict the accuracy of the proposed system. The most critical step for classification is to find out the specific machine learning algorithm which will result in highest accuracy for the given dataset. As a result, we evaluated a handful of classification techniques including logical/symbolic technique like decision trees, ensembles of classifiers techniques using random forest, instance based learning technique named k-nearest neighbor and finally the supervised machine learning technique named Support Vector machine (SVM).

- Support Vector Machine (SVM)

First, we have applied the widely used and state-of the art classifier, named SVM classifier, which is the newest supervised machine learning classification technique. In binary classification, SVM creates a hyperplane that separates data from two different classes. The largest possible distance is created between the separating hyperplane by maximizing the margin, thus creating the separation [86].

The choice of kernel determines the separation boundary of the classes. Radial Basis Function (RBF) or Gaussian kernel are popular algorithms to use as default kernels for any non-linear model. RBF is defined as:

$$K(x, x') = \exp(-\gamma ||x - x'||^2) \dots\dots\dots\dots\dots\dots\dots\dots\dots\dots\dots\dots(5)$$

where x and x' are two training samples of the feature space and γ determines the influence of the squared Euclidian distance between the feature vectors x and x' to build the hyperplane. Quadratic and cubic kernels are polynomial kernels with degrees of 2 and 3, respectively. Polynomial kernels are defined by

$$K(x,y) = (x^T y + c)^d \dots\dots\dots\dots\dots\dots\dots\dots\dots\dots\dots\dots\dots\dots\dots\dots\dots(6)$$

where x and y are vectors in the input space (*i.e.,* vectors of features computed from training or test samples) and c (≥ 0) is a free parameter trading off the influence of higher-order versus lower-order terms in the polynomial. It is generally not advised to consider higher order polynomials because they tend to over-fit the data.

- K Nearest Neighbor

The next classification technique applied was an instance-based statistical method, kNN. This technique is based on the principle that the instances of a dataset will exist in close proximity to other instances that have similar properties [87][86][89][95][94][94][94][95]. In this method, a test example is classified by observing the class label of its nearest neighbors. The kNN locates the k nearest instances to the query instance and determines its class by identifying the single most frequent class label. A distance metric is generated by calculating the relative distance between the objects. The objects under the same classification label will have the minimum distance while the distance will be maximum for objects under different classes. A list of distance metrics calculation approaches is shown in table II.

Table 8 Distance matrices for kNN

Methods	Equation
Minkowsky	$D(x,y) = \left(\sum_{i=1}^{m} \lvert x_i - y_i \rvert^{\,r} \right)^{1/r}$
Manhattan	$D(x,y) = \sum_{i=1}^{m} \lvert x_i - y_i \rvert$
Chebychev	$D(x,y) = {}_{i=1}^{m}max \lvert x_i - y_i \rvert$
Euclidean	$D(x,y) = \left(\sum_{i=1}^{m} \lvert x_i - y_i \rvert^{2} \right)^{1/2}$
Camberra	$D(x,y) = \sum_{i=1}^{m} \dfrac{\lvert x_i - y_i \rvert}{\lvert x_i + y_i \rvert}$
Kendall's Rank Correlation:	$D(x,y) = 1 - \dfrac{2}{m(m-1)} \sum_{i=j}^{m} \sum_{j=1}^{i-1} sign(x_i - x_j)sign(y_i - y_j)$

The performance of the KNN classifier depends on the choice of k. Since there is no principled way to choose k, sometimes the algorithm can run poorly. Also another major disadvantage of this system is large computational time.

- Decision Tree

Decision trees, a hierarchical classifier method, is the simplest and most widely used logic-based classification technique. In this approach, the test data is classified by sorting as trees based

on their feature values. The node of the decision tree is the feature of the test data to be classified and the branches represent a value that the node can predict. Various efficient algorithms have been developed to construct a reasonably accurate decision tree such as Hunt's algorithm [88], Gini's diversity index method, and relief algorithm [89]. Once the decision tree is developed, the unknown feature values from test data is then passed down to all branches of the node to detect the unknown class distribution. The output is the combination of different class distribution that sum to 1. Decision tree mainly performs better for categorical features but does not perform well when classes have multimodal distribution.

- Random Forest

A random forest is composed of a large number of decision trees which are mainly used to correct the overfitting problem of decision trees [90]. In this technique, multiple decision trees, trained from different subsets of the same training set, are averaged and overfitting is avoided by reducing the variance of the system, which eventually increases the performance of the final model. The training algorithm works by applying bootstrap aggregating, or bagging techniques, to tree learners. For example, if a training set x = x1, ..., xn has responses y = y1, ..., yn, applying bagging will repeatedly select a random sample with replacement of the training set for B different times and will fit the trees to these samples. Now for b = 1,..., B, if we call each different samples from n training examples of x and y as xa and xb, then the decision tree need to be trained for these xb and yb. Once the model is trained, predictions for unseen samples or test set x' can be generated by calculating the average of the predictions from all the individual decision trees using (2):

$$\tilde{f} = \frac{1}{B} \sum_{b=1}^{B} \hat{f}_b(x')$$

CHAPTER 3

RESULTS AND DISCUSSION

3.1   Results

3.1.1   Tremor Measurement

As we have done two different study for tremor, results with subjects emulating tremor following by results with clinical trial where 19 PD patients have been participated.

3.1.1.1   Study with subjects emulating tremor

The results from the calculation of extracted features for the different severities of resting and postural tremor are listed in Fig 14. It is shown in the figure that the value of every feature increases as tremor severity increases. The first two and second two columns depict resting and postural tremor results, respectively. The position of the sensor (index finger or wrist) alternates with each column starting with the finger position. Rows one to three are gyroscope feature results: 1. Natural logarithm of the root mean square of angular velocity; Log(RMS (Ang. Vel.)) 2. Natural logarithm of gyroscope peak power; Log(Gyro Power) 3. The standard deviation of angular velocity; Stdev(Ang. Vel.). Rows four to six are accelerometer feature results: 4. Natural logarithm of the root mean square of linear acceleration; Log(RMS (L. Accel.)) 5. Natural logarithm of

accelerometer peak power; Log(Accel Power) 6. The standard deviation of linear acceleration; Stdev(L. Accel.).

The classification accuracy of the resting and postural tremor severity quantification models for different combinations of features are shown in Table 8. The different combinations of features were selected based on the placement of sensor on the body (index finger and wrist) as well as sensor type (gyroscope and accelerometer). For example, when the features calculated from both sensors fixed on the index finger were used to train the classifier, it achieved a classification accuracy of 88.9% (column 3, row 4) for resting tremor and 82.1% (column 4, row 4) for postural tremor. However, when the classifier was trained with all the features calculated from both sensors on both the index finger and wrist, the accuracy was 83.3% (column 3, row 10) for resting tremor and 79.5% (column 4, row 10) for postural tremor. In total, the classifier performance for all the sensors and locations were computed separately and together (Table 8).
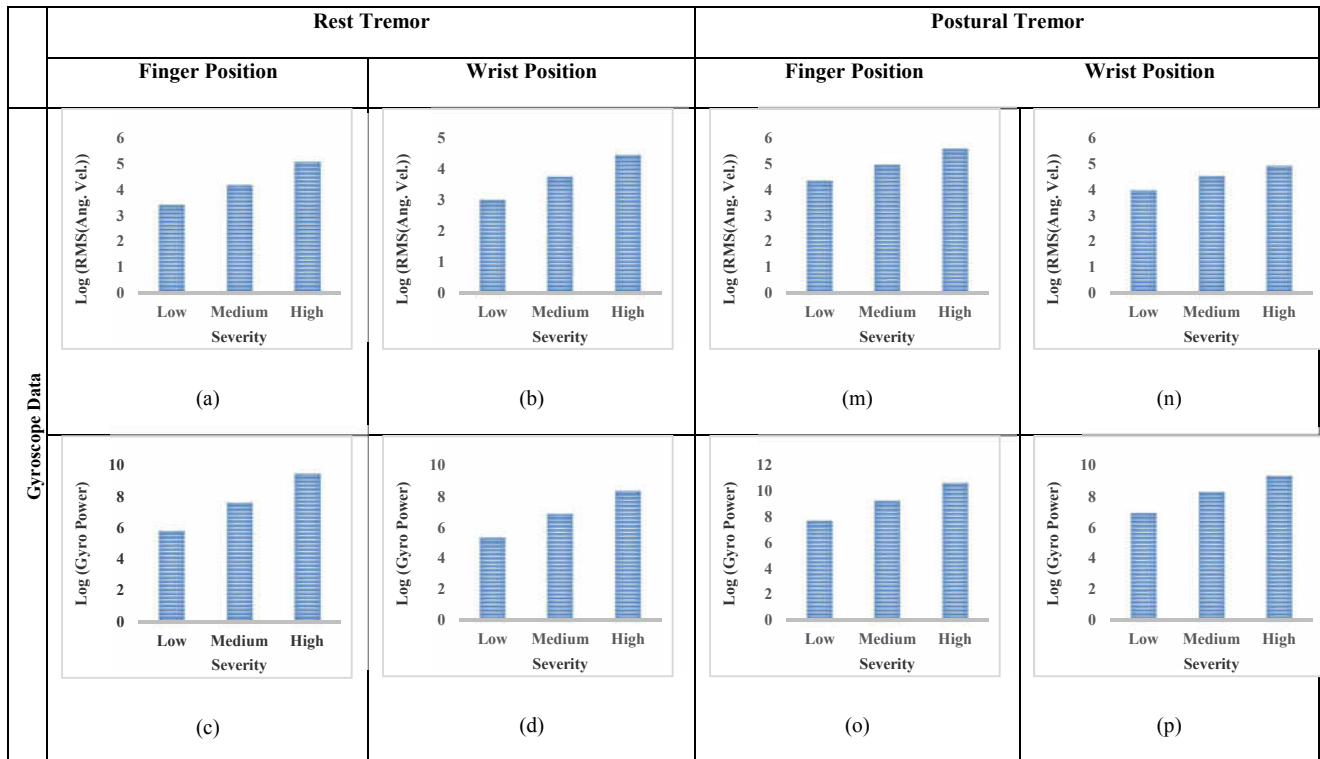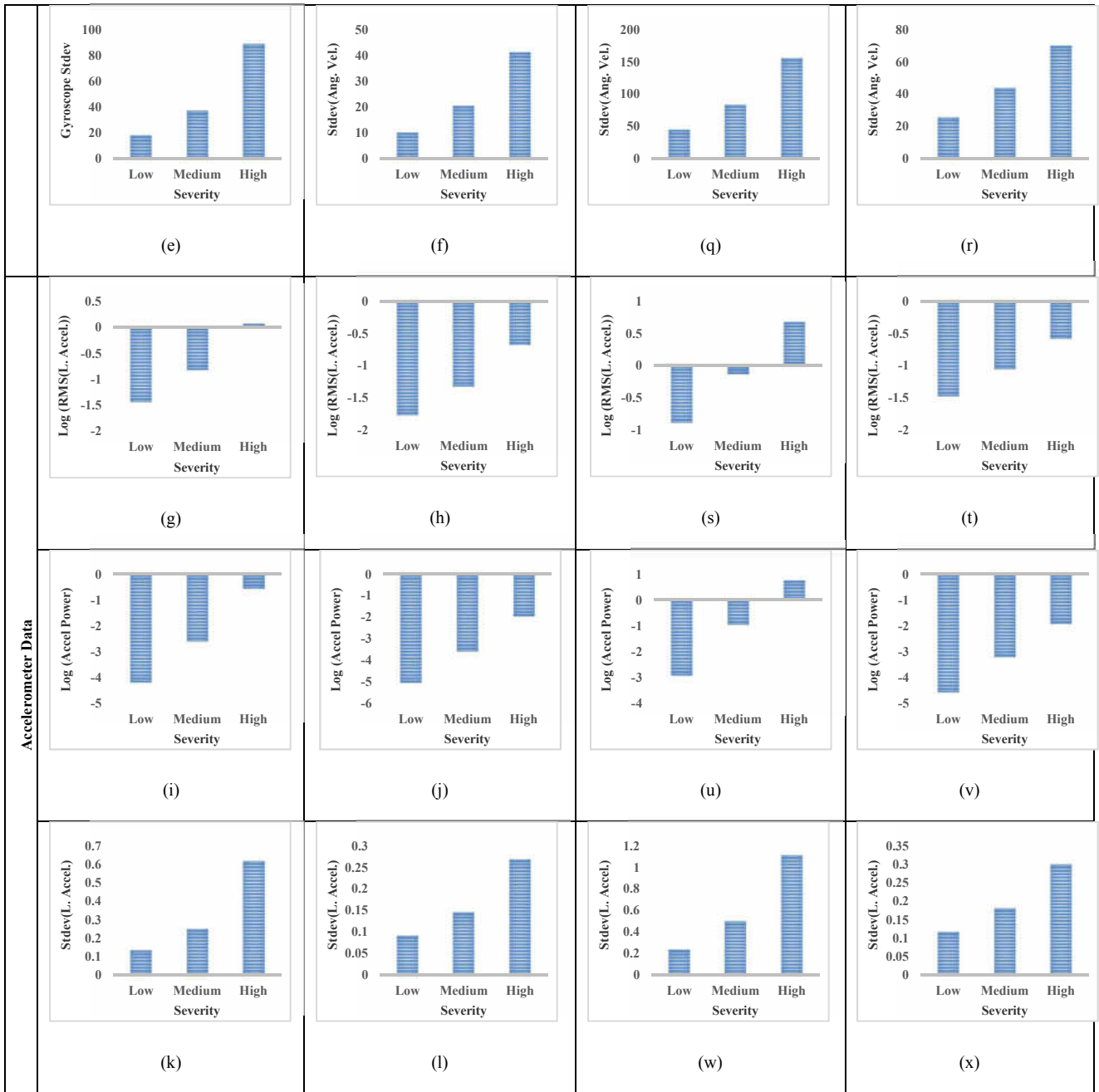
Figure 13. Severities of resting and postural tremor. Tremor severity variation of the 12 features extracted when the sensor is placed on both the wrist and finger position are displayed in the figure range a-l and m-x for rest and postural tremor, respectively.

Table 9. Resting and postural tremor severity quantification

SENSOR PLACEMENT	SENSOR	REST TREMOR	POSTURAL TREMOR
Finger	Accelerometer	80.6%	79.5%
	Gyroscope	88.9%	59.0%
	Accelerometer + Gyroscope	88.9%	82.1%
Wrist	Accelerometer	77.8%	48.7%
	Gyroscope	50%	53.8%
	Accelerometer + Gyroscope	80.6%	53.8%
Finger + Wrist	Accelerometer	86.1%	84.6%
	Gyroscope	86.1%	69.2%
	Accelerometer + Gyroscope	83.3%	79.5%

Furthermore, the effect of standard deviation of accelerometer and gyroscope values on overall classification accuracy was determined. When the standard deviation feature was excluded from the index finger analysis, the classifier achieved a classification accuracy of 86.1% and 78.8%, compared to the 88.9% and 81.8% accuracy achieved when it was included for resting and postural tremor, respectively.

3.1.1.2   Results with clinical trial of PD patients

3.1.1.2.1   Resting Tremor

All the parameter value computed for each of the subjects are shown in Table 10 . Each feature has two values computed while signals acquired before and signals captured after medication resting tremor task. UPDRS scores of the resting tremor for both before and after taking medication had been taken by a clinician. As shown in Table 10 , each feature values (before medication and

after medication) were colored either green or red. Feature values were colored green on when changes in On medication value is consistent with changes in UPDRS scores. It could happen in two possible scenarios. First, when there is a change of less than 10 % for On medication value with Off medication value and UPDRS scores are same for both before and after medication. Also, the feature values remained green if On medication value changes more than 10 % with respect on Off medication value and there is a change in UPDRS scores for before and after medication. From the table 10, it can be seen that dominant frequency parameter values for finger resting tremor are colored red for several subjects as the feature values are not consistent with UPDRS scores for 5 subjects. So it is colored red for that values in rows corresponding to those subjects..

Also, classification diagram for finger tremor is listed in figure 15. Rows 0, 1, 2 specifies the number of subjects that has tremor of UPDRS scores of 0, 1 and 2 respectively. Column 0, 1 and 2 indicates the number of subjects that has been predicted as UPDRS scores of 0, 1 and 2 respectively. Green color in the rectangle box in the figure means UPDRS score has been reported perfectly while red score means the subject tremor severity score predicted does not match with ground truth.

Table 10. Before and after medication feature values for finger tremor (resting). Feature values were colored green on when changes in On medication value is consistent with changes in UPDRS scores. Features were colored red when when changes in On medication value is not consistent with changes in UPDRS scores

Subject Number	Number of Tremor Window		Peak Power/Total Power (Ratio)		Dominant Frequency		Amplitude		UPDRS Score	
	Before Medication	After Medication	Before Medication	After Medication	Before Medication	After Medication	Before Medication	After Medication	Before Medication	After Medication
2	0	0	0.43	0.43	4.96	5.11	1.07	1.01	0	0
3	0	0	0.40	0.44	2.12	3.94	1.6	1.53	0	0
4	3	0	0.70	0.52	3.96	3.40	2.12	1.91	1	0
5	1	0	0.58	0.47	4.51	3.12	2.12	1.87	1	0
6	0	1	0.49	0.52	3.96	4.11	1.45	1.39	0	0
7	0	0	0.47	0.51	3.94	4.64	1.29	1.23	0	0
8	0	0	0.41	0.42	3.42	3.51	1.44	1.38	0	0
9	0	0	0.44	0.47	3.12	4.90	1.46	1.61	0	0
10	0	0	0.39	0.42	2.69	2.73	1.63	1.58	0	0
11	9	9	0.92	0.88	5.07	5.07	2.9	2.85	2	2
12	0	0	0.39	0.49	3.81	4.59	1.59	1.78	0	0
13	0	0	0.46	0.44	3.36	3.4	1.39	1.44	0	0
14	6	4	0.71	0.68	4.29	4.03	2.62	1.61	2	1
15	9	5	0.88	0.75	4.42	3.94	3.3	1.93	2	1
16	0	0	0.41	0.40	2.51	2.58	1.61	1.49	0	0
18	2	2	0.61	0.61	3.40	3.27	1.78	1.66	1	1
19	6	9	0.65	0.67	5.46	5.55	3.22	3.45	1	1
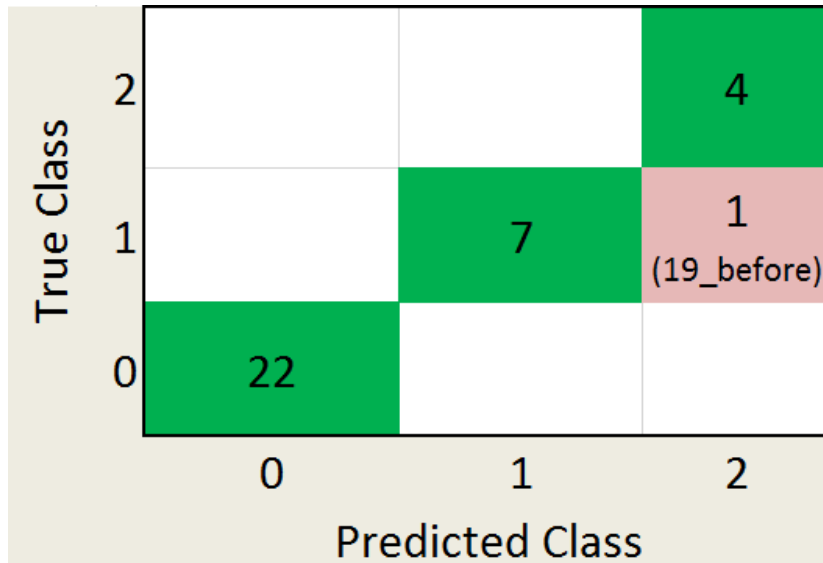
Figure 14. Finger tremor classification with SVM 5 fold cross validation

Table 11 : Classification accuracy across different classifier for finger tremor

Classifier	Accuracy	Sensitivity	Specificity	AUC
SVM (Linear)	97.10%	96.33%	97.87%	0.99
kNN	91.20%	90.67%	91.73%	0.94
Decision tree	88.20%	88.33%	88.07%	0.93
Random Forest	82.40%	69.33%	95.47%	0.9

Different extracted Parameter values for tremor analyzed from wrist position are shown in Table 12. Classification results based on the selected features are presented in Figure 16.

Table 12. Before and after medication feature values for wrist tremor (resting). Feature values were colored green on when changes in On medication value is consistent with changes in UPDRS scores. Features were colored red when when changes in On medication value is not consistent with changes in UPDRS scores

Subject Number	Number of Tremor Window	Peak Power/Total Power (Ratio)	Dominant Frequency	Amplitude	UPDRS Score

	Before Medication	After Medication	Before Medication	After Medication	Before Medication	After Medication	Before Medication	After Medication	Before Medication	After Medication
2	0	0	0.56	0.53	3.59	3.77	1.17	1.09	0	0
3	0	0	0.38	0.40	3.52	3.68	1.16	1.13	0	0
4	1	0	0.56	0.43	4.42	3.94	1.32	1.18	1	0
5	3	0	0.50	0.43	3.67	3.10	2.02	1.37	1	0
6	8	2	0.73	0.52	4.29	4.16	1.49	1.37	0	0
7	1	0	0.47	0.48	4.49	4.54	1.21	1.13	0	0
8	0	0	0.40	0.39	4.33	3.94	1.37	1.33	0	0
9	0	0	0.44	0.40	2.95	4.29	2.04	2.01	0	0
10	0	0	0.39	0.47	2.60	2.76	1.13	1.18	0	0
11	9	9	0.95	0.95	5.11	5.07	2.67	2.65	2	2
12	0	0	0.45	0.46	4.20	5.07	1.45	1.5	0	0
13	0	0	0.37	0.39	3.11	3.27	1.11	1.17	0	0
14	4	3	0.54	0.51	5.11	4.29	1.3	0.9	2	1
15	8	4	0.81	0.75	4.51	3.86	2.91	2.45	2	1
16	0	0	0.46	0.40	4.81	3.81	0.88	0.93	0	0
18	2	2	0.54	0.52	3.51	3.48	1.13	1.08	1	1
19	2	2	0.55	0.52	4.60	3.48	1.15	1.08	1	1
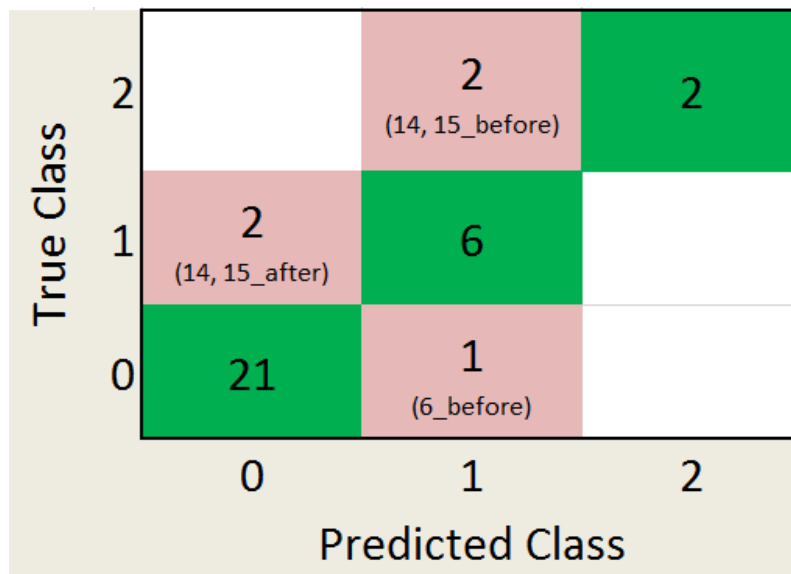
Figure 15. Wrist tremor classification with 5 fold cross validation

Table 13 Classification accuracy across different classifier for wrist tremor

Classifier	Accuracy	Sensitivity	Specificity	AUC
SVM (Linear)	**85.30%**	**86.00%**	**84.60%**	**0.93**
kNN	**82.40%**	**83.67%**	**81.13%**	**0.86**
Decision tree	**79.40%**	**72.33%**	**86.47%**	**0.77**
Random Forest	**79.40%**	**81.67%**	**77.13%**	**0.8**

3.1.2   Bradykinesia

Like tremor analysis two different study has been done and results from two studies would be mentioned here:

3.1.2.1   Results with Subjects Emulating PD Bradykinesia

Table 14 shows the statistically significant features of x-axis gyroscope data for all 4 UPDRS scores. Sample entropy, and Lyapunov exponents were not significantly different.

Figure 17 represents the 4 UPDRS score trials based on the two most significant features named the activity and Hurst component.
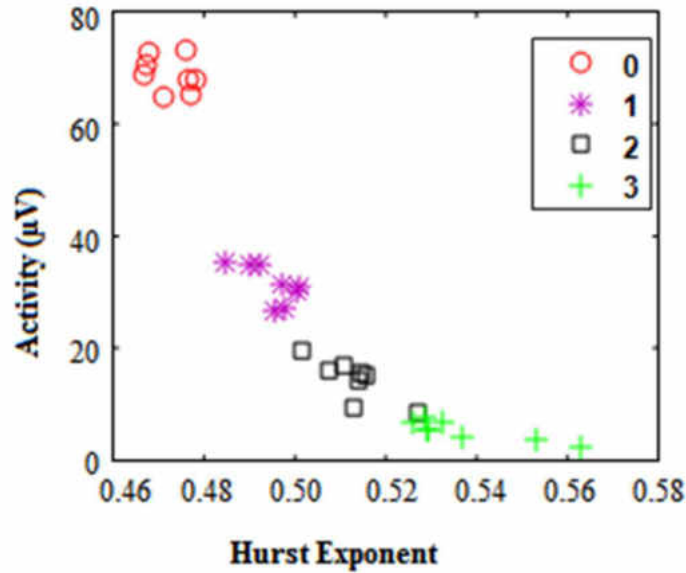
Figure 16. Four UPDRS scores representation based on activity and Hurst exponent.

Table 15 shows the classification accuracy achieved through multiclass SVM classification using a Gaussian kernel function:

Table 14. Statistically significant features of x-axis gyroscope data

UPDRS Score	Approximate Entropy	Activity	Mobility	Complexity	Hurst exponent	Maximum Power	Total Power
0	0.23±0.029*	68.9±29.0*	0.29±0.03*	0.82±0.09*	0.47±0.004*	206872.8±2008.7*	887506.5±45521.9*
1	0.26±0.012*	31.4±32.2*	0.24±0.01*	0.73±0.07*	0.49±0.005*	95601.2±1819.1*	706666.5±16902.4*
2	0.31±0.022*	14.1±35.4*	0.22±0.01*	0.73±0.05	0.51±0.007*	59060.5±1998.2*	411477.2±81817.9*
3	0.34±0.052*	5.41±16.5*	0.21±0.01	0.67±0.05*	0.54±0.013*	21031.8±676.4*	244139.6±84753.7*

Table 15. Classification accuracy with multiclass SVM classification

UPDRS Score	Accuracy	Sensitivity	Specificity	AUC
0	100%	100%	100%	1

1	100%	100%	100%	1
2	94%	100%	88%	0.99
3	95%	90%	100%	0.99
Overall	97.25%	97.5%	97%	0.995

3.1.2.2 Trial with PD patients

Bradykinesia parameter for finger tapping task is shown in table 16. Also classification diagram for the finger-tapping is listed in figure 18 Rows 0,1,2 and 3 lists the number of subjects that has tremor of UPDRS scores of 0, 1, 2 and 3 respectively. Column 0, 1, 2 and 3 lists the number of subjects that has been predicted as UPDRS scores of 0, 1 and 2 and 3 respectively. As like Table 10, green color in Table 16 and Table 18 means UPDRS score has been reported perfectly. Red color indicates that feature values are not consistent with UPDRS scores.

Table 16. Bradykinesia finger-tapping features. Feature values were colored green on when changes in On medication value is consistent with changes in UPDRS scores. Features were colored red when when changes in On medication value is not consistent with changes in UPDRS scores

No.	Number of Tapping		Tap time(s)		Average Closing Acceleration (m/s^2)		Average Opening Angular Velocity (degree/second)		Average Closing Angular Velocity (degree/second)		Standard Deviation of Tap time (s)		Number of hesitation		UPDRS Score	
	BM	AM	BM	AM	BM	AM	BM	AM	BM	AM	BM	AM	BM	AM	BM	AM
2	64	71	0.45	0.41	0.85	0.55	318	243	342	245	0.04	0.04	3	0	0	0
3	90	104	0.33	0.28	5.04	5.33	1017	1530	1246	1294	0.04	0.02	3	3	1	0
4	37	53	0.81	0.6	2.14	3.1	404	835	548	841	0.18	0.06	4	4	2	1
5	70	68	0.42	0.44	4.38	5.88	778	1248	871	972	0.03	0.03	9	6	1	0
6	95	127	0.31	0.23	5.39	4.31	369	240	762	524	0.07	0.08	6	5	1	1

7	99	88	0.26	0.32	2.65	3.88	529	1021	574	1015	0.15	0.03	3	2	2	0
8	87	114	0.33	0.25	4.93	5.73	549	921	1002	1369	0.07	0.08	4	4	1	1
9	87	105	0.33	0.28	6.8	6.4	657	582	1167	964	0.09	0.19	1	2	1	2
10	34	51	0.91	0.57	1.41	1.84	1556	1861	1206	1503	0.14	0.05	2	5	2	1
11	57	84	0.51	0.34	3.39	5.19	1201.1	1225.5	1212.6	1088.33	0.08	0.06	2	0	1	1
12	31	26	0.99	1.22	0.71	0.8	276.08	260.47	164.63	171.81	0.45	0.26	2	2	3	3
13	39	48	0.76	0.64	2.31	3.14	534	768	670	867	0.15	0.1	3	1	2	1
14	56	42	0.48	0.67	3.13	1.24	426.01	208.93	501.54	226.54	0.44	0.19	3	0	3	2
15	70	39	0.43	0.77	0.833	1.61	239.49	834.98	315.85	1039.34	0.25	0.15	4	2	2	1
16	96	81	0.3	0.37	4.23	7.4	898.52	1191.8	1013.3	1242.3	0.03	0.01	2	0	0	0
18	64	71	0.46	0.41	2.64	2.83	717.64	761	649.95	727	0.18	0.06	2	1	2	1
19	47	53	0.64	0.56	1.38	2.31	499.72	460.74	393.95	427.41	0.48	0.5	1	1	3	3

* BM: Before Medication; AM: After Medication
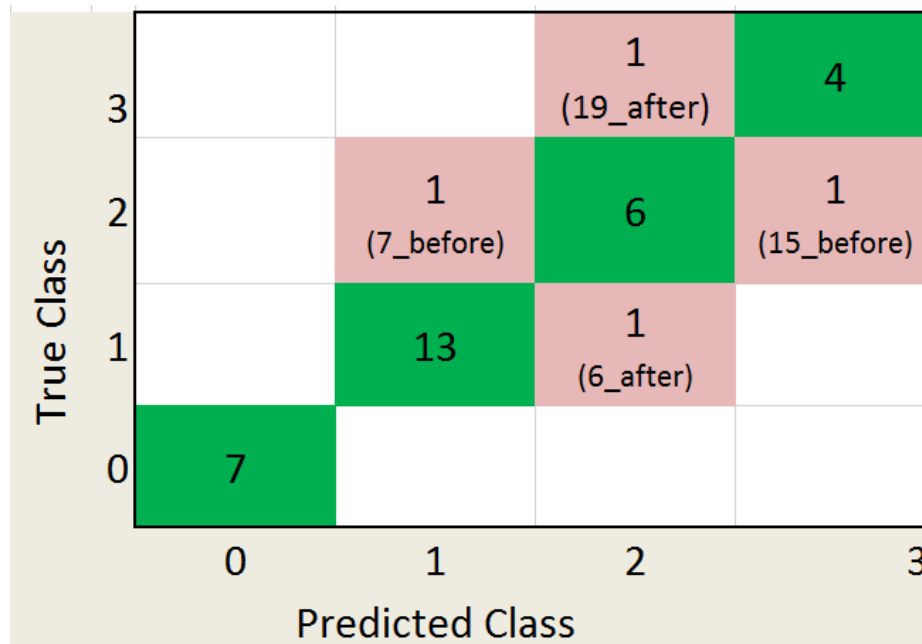
Figure 17. Finger tapping classification with 5 fold cross validation

Table 17 Classification accuracy across different classifier for finger tapping

Classifier	Accuracy	Sensitivity	Specificity	AUC
SVM (Linear)	88.20%	90.75%	85.65%	0.89
kNN	64.70%	70.75%	58.65%	0.66
Decision tree	58.80%	67.00%	50.60%	0.59
Random Forest	82.45%	80.25%	84.65%	0.84

Table 18. Bradykinesia hand grasping features. Feature values were colored green on when changes in On medication value is consistent with changes in UPDRS scores. Features were colored red when when changes in On medication value is not consistent with changes in UPDRS scores

No.	Number of Grasping		Grasp time (sec)		Average Closing Acceleration (m/s^2)		Average Opening Angular Velocity (deg/sec)		Average Closing Angular Velocity(deg/sec)		Standard Deviation of Grasp time (sec)		Number of hesitation		UPDRS Score	
	BM	AM	BM	AM	BM	AM	BM	AM	BM	AM	BM	AM	BM	AM	BM	AM
2	65	42	0.46	0.6	5.04	2.94	1009	849	1499	1385	0.05	0.04	1	1	0	0
3	46	51	0.64	0.58	1.32	1.68	1171	1446	856	994	0.05	0.04	1	3	0	0
4	36	53	0.56	0.38	1.6	1.78	1647	1992	1593	1637	0.12	0.06	4	2	2	0
5	42	55	0.66	0.49	1.88	3.55	928	951	1183	1360	0.05	0.07	3	2	0	0
6	53	77	0.53	0.41	2.01	1.48	422	602	601	792	0.05	0.06	6	2	1	0
7	75	119	0.4	0.25	2.25	3.88	756	1162	773	1201	0.05	0.05	3	2	0	0
8	56	60	0.53	0.5	1.98	2.97	1245	1426	768	850	0.17	0.08	2	2	1	0
9	63	59	0.45	0.5	3.79	3.04	1167	1042	1515	1260	0.09	0.06	1	2	0	1
10	50	53	0.64	0.57	2	1.97	1818	1766	1643	1637	0.04	0.05	2	7	0	0
11	59	69	0.48	0.42	1.47	1.99	1524	1754	1483	1853	0.08	0.07	2	0	2	1
12	17	20	1.71	1.55	0.47	0.76	294	472	129	284	0.33	0.13	2	2	3	3

13	58	61	0.51	0.48	2.06	2.08	594	588	634	654	0.11	0.1	1	1	1	1
14	40	50	0.56	0.46	3.04	2.81	644	664	903	892	0.43	0.38	3	0	2	2
15	31	42	0.99	0.71	1.14	1.27	1063	1684	1313	1808	0.2	0.15	4	2	2	1
16	85	87	0.35	0.33	2.05	2.13	1055	1101	1237	1261	0.08	0.02	2	0	0	0
18	57	57	0.52	0.51	0.73	0.59	1513	1875	1438	1802	0.18	0.06	2	1	0	0
19	34	42	0.98	0.72	1.18	1.28	1052	1701	1300	1826	0.20	0.15	4	3	2	1

* BM: Before Medication; AM: After Medication

During the trial PD patients showed different severities of bradykinesia symptoms both before and after taking medication. There were total 32 trials for 16 subjects if we count both before taking PD medication and after medication trial. UPDRS score 0, 1, 2, 3 scores were observed by clinician during finger tapping task. Four class classification was performed. For training the classifier, 7 subjects showing no symptoms of bradykinesia are classified as zero. Class 1 and Class 2 consists of features extracted from 14 subjects and 8 subjects respectively. Class 3 consists of 3 subjects parameters. Then five-fold cross validation accuracy was performed on the feature dataset and initially 65.5% classification accuracy was achieved. Features included in the training dataset was: Number of tapping, mean tap time, average closing acceleration, average opening angular velocity and average closing angular velocity.
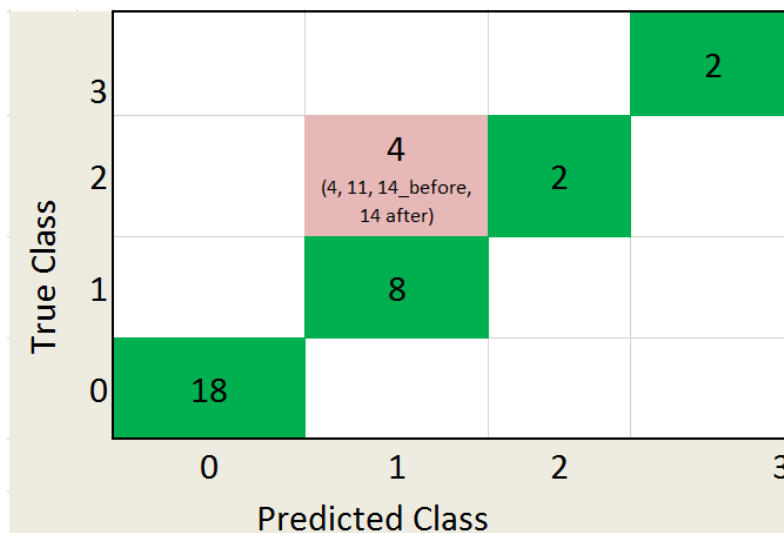
Figure 18. Hand grasping classification with 5 fold cross validation

After this number of tapping feature was removed and hesitation and standard deviation of tap time was included in the feature training dataset and accuracy was increased from 65.1% to 85.5%. The classification result is shown in figure.

As similar with finger tapping, table 18 highlights the feature values for hand grasping.

Table 19 Classification accuracy across different classifier for hand grasping

Classifier	Accuracy	Sensitivity	Specificity	AUC
SVM (Linear)	88.20%	88.25%	88.15%	0.89
kNN	82.40%	83.50%	81.30%	0.87
Decision tree	85.30%	83.25%	87.35%	0.83
Random Forest	85.30%	82.50%	88.10%	0.85

3.1.3 Gait

Three different study has been done for gait analysis of PD patients. Results section would include results for each of the study.

3.1.3.1 Gait Speed Measurement.

The estimation accuracy of KF for various values of $\in, \delta, \lambda$ and μ is shown in Table 20. The values were changed from $1e^{-2}$ to $1e^{-6}$ gradually. As illustrated in Table I, the best estimation accuracy was obtained while the values of $\in, \delta, \lambda$ and μ were set to $1e^{-5}$.

Once the best performance of KF was deduced, the system performance for various speeds was examined. The results obtained for various speeds are listed in Table 21, which shows the calculated speed before and after Kalman filter along with the measured mean squared error.

Table 20. Performance of KF for different G and Q matrices

Case	G and Q Matrices	Mean Square Error	Estimation Performance
1	$\epsilon = \delta = \lambda = \mu = 1e^{-2}$	5.76	Poor
2	$\epsilon = \delta = \lambda = \mu = 1e^{-3}$	1.96	Poor
3	$\epsilon = \delta = \lambda = \mu = 1e^{-4}$	1.21	Poor
4	$\epsilon = \delta = \lambda = \mu = 1e^{-6}$	0.36	Good
5	$\epsilon = \delta = \lambda = \mu = 1e^{-5}$	0.18	Very Good

Table 21. Speed estimation from inertial measurement unit data

Actual Speed (mile/hour)	Time (second)	Distance Traveled (meter)	Estimated Speed (mile/hour)	Mean square Error	Estimated Speed with Kalman Filter (mile/hour)	Mean Square Error
0.50	60	13.38±0.35	0.60±0.086	1.60	0.55±0.087	0.40
1.00	60	26.82±0.71	0.92±0.080	1.02	0.97±0.055	0.10
2.00	60	53.64±1.41	1.93±0.056	1.10	1.96±0.071	0.25
3.00	60	80.46±2.12	2.91±0.091	1.30	2.94±0.067	0.18
			Average MSE Error =	1.26	Average MSE Error =	0.23

Table 16 shows that the implementation of KF helps to reduce noise on the estimated speed for all four sets of speeds. The MSE was reduced by 75% for 0.5 mile/hour; 90% for 1 mile/hour; 77% for 2 mile/hour and 86% for 3 mile/hour. The best estimation accuracy was exhibited by 1 mile/hour speed with a mean squared error of estimation equal to 0.10 only. The average mean square error reduced by 82% for all four different speeds.

3.1.3.2 Parkinson gait using Physilog

Table 22 shows the features extracted from patients gait signal using Physilog software. As like previous case, Value colored green are for those parameters whose change in value after medication is consistent with change in UPDRS scores after medication.

Table 22. Gait feature values before and after medication. Feature values were colored green on when changes in On medication value is consistent with changes in UPDRS scores. Features were colored red when when changes in On medication value is not consistent with changes in UPDRS scores

No.	Speed (m/s)		Variability (%)		Stance (% of gait cycle)		Swing (% of gait cycle)		Foot Flat (% of stance)		Strike angle (deg)		Lift -off Angle (deg)		UPDRS Score	
	BM	AM	BM	AM	BM	AM	BM	AM	BM	AM	BM	AM	BM	AM	BM	AM
2	0.77	0.89	2.69	3.65	67.38	63.68	32.62	36.02	61.03	53.55	23.47	28.16	53.22	59.14	2.88	1.82
3	1.28	1.67	3.56	4.22	58.96	51.68	33.04	43.32	61.58	53.84	22.29	28.65	59.64	70.15	3.29	1.36
4	0.95	1	3.8	4.61	62.71	67.29	33.29	37.71	59.36	59.71	12.39	8.75	56.75	51.71	1.83	2.29
5	1.16	1.21	2.59	4.57	63.55	63.98	32.45	34.02	57.54	56.29	22.6	22.79	62.7	64.48	1.82	1.15
6	0.92	0.98	3.85	1.93	67.24	65.5	32.76	34.6	64.27	60.33	17.49	19.15	62.19	67.65	3.93	2.52
7	1.49	1.52	1.5	1.36	59.14	58.36	40.86	41.64	56.93	56.57	24.25	26.39	59.57	61.15	1.35	1.27
8	1.2	1.34	1.79	1.4	58.38	51.07	39.62	47.93	60.11	68.24	13.2	17.38	49.56	57.36	2.46	2.03
9	1.14	1.15	5.73	5.33	59.07	58.44	40.93	41.56	67.07	64.67	24.87	24.44	63.21	63.99	2.44	1.41
10	1.04	0.99	3.3	2.94	66.26	66.76	33.74	33.24	58.11	58.53	17	15.13	64.3	61.41	2.10	2.89
11	0.86	0.87	2.11	2.92	60.2	60.52	39.8	39.48	53.83	52.58	17.68	18.32	61.42	63.75	4.32	4.29
12	0.91	0.97	4.1	1.9	61.7	56.51	38.3	43.49	50.71	52.65	10.97	19.05	55.59	49.49	3.62	3.12
13	0.54	0.86	2.89	5.15	65.74	59.1	34.26	40.9	69.47	55.62	4.1	7.47	47.99	57.86	3.98	5.51
14	1.13	1.15	0.95	2.86	63.71	64.26	36.29	35.74	59.36	57.63	17.74	19.87	58.37	58.35	2.56	2.70
15	1.01	1.14	4.59	3.85	69.56	61.63	42.31	38.37	64.53	61.02	27.67	32.45	63.71	72.44	2.59	1.42

16	1.53	1.56	1.57	1.56	54.57	54.26	45.43	45.74	51.07	54.1	24.22	23.49	72.89	72.43	1.33	1.30
18	1.28	1.25	3.23	9.39	56.09	57.25	43.91	42.75	64.53	64.38	25.44	26.49	55	56.47	2.52	2.14
19	1.52	1.56	1.57	1.36	59.31	58.9	40.69	42.7	49.63	47.08	41.71	42.19	73.97	73.19	1.90	1.41

* BM: Before Medication; AM: After Medication

Classification performance of the extracted parameters are shown in figure Classification accuracy of 85.2% is achieved after excluding features average swing time and variability.

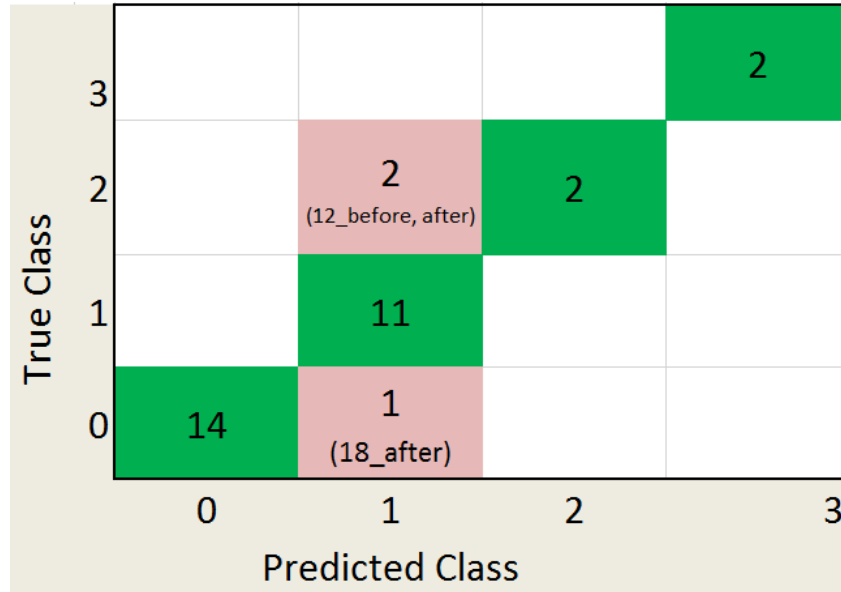**Figure 19. Gait classification accuracy with SVM 5 fold cross validation**

Table 23 Classification accuracy across different classifier for Gait

Classifier	Accuracy	Sensitivity	Specificity	AUC
SVM (Linear)	87.50%	86.50%	88.50%	0.89
kNN	65.70%	62.50%	68.90%	0.69
Decision tree	84.40%	85.75%	83.05%	0.88
Random Forest	84.40%	84.50%	84.30%	0.86

3.2 Discussion

In this report, signal processing and machine learning method for tremor, bradykinesia and gait analysis were discussed.

3.2.1 Tremor

Tremor verification was performed in two different setting. First with mock patients to design the algorithm, and with actual PD patients.

For the mock patient tremor quantification study, different features derived from multiple sensor signals and the effect of sensor placement on tremor severity classification was investigated. From Table 9, it is seen that in case of both resting and postural tremor, classifier performance was increased when it was trained on features extracted from only the index finger tremor signal rather than the combination of the index finger and the wrist tremor signals. This leads to the conclusion that the index finger is a significant appendage for tremor data classification when considering that both the index finger and the wrist are the main affected body locations.

Furthermore, two of the features used had been shown to correlate well with UPDRS tremor scores according to previous work [47]. In addition, this study investigated the standard deviations of angular velocities or linear accelerations as a metric to classify tremor severity which gave encouraging results. In both resting and postural tremor categories, classification accuracy was reduced when it was excluded as a parameter in the analysis.

In the second step of tremor quantification, we have verified our algorithm performance by collecting signals from actual PD patients. Features that were used to quantify resting tremor are mentioned in table 10 and table 12. As green colors were indicate that the feature values for before and after medication trend consistently with UPDRS scores obtained from the clinician before and after medication, we can see that almost all the features except average dominant frequency

trended according to UPDRS scores. So Dominant frequency was excluded from the machine learning training dataset. However, dominant frequency is an important parameter which is required to find out the number of tremor window as to be qualified as a tremor window, dominant frequency has to be in the range from 3-7 Hz. For only subject 12, three out of four parameters did not trend with UPDRS score as after medication value for those parameters changed more than 10% while UPDRS score before and after medication remains zero. Classification accuracy of resting tremor for signals acquired from finger position is shown in Figure 11 and wrist position is shown in Figure 13. It can be observed that more prediction accuracy is achieved (more than 9%) case of resting tremor for finger position than for wrist position. We believe prediction accuracy of finger tremor 96.9% is actually quite high although UPDRS scores obtained from clinician may also suffer from subjective bias which may vary the prediction accuracy slight upwards or downwards. Also, from Figure 13 we can see that only one subjects misclassified however with scale of one and in PD, difference of UPDRS score is just one is not much significant. with finger tremor. Also it can be noted that finger is more sensitive limb than wrist for tremor severity prediction.

Same parameter was also obtained for postural tremor. However, very few patients exhibits postural tremor according to UPDRS score obtained by clinician. It is consistent with the knowledge that resting tremor is more evident in PD tremor and postural tremor is more dominant in essential tremor patients. As can be seen from feature table, very few patients showed trend with UPDRS score. However, Only patients who showed significant tremor (UPDRS score of 2) both before and after medication, the parameter trend very well for the subject which showed the extracted features effectiveness. One important point to add that our method of finding dominant axis has achieved our calculation to be insensitive to placement of sensor axis in limb. As the

algorithm would always choose axis that shows maximum change in value with time, need for combining all axis value is eliminated. If all the axis value was instead combined important information would be lost.

3.2.2 Bradykinesia

Bradykinesia assessment was also done with two sets of datasets.: first with the mock patients data and second with the real PD patients.

For mock patient dataset analysis, the goal of the study was to develop an efficient bradykinesia assessment system using simulated data acquired from IMU placed on the index finger. Table 14 lists the set of linear and nonlinear features found to be significantly different for various level of bradykinesia. The approximate entropy and Hurst exponent increased significantly from UPDRS score 0 to 3. The observation of a gradual increase of approximate entropy implied a gradual rise of complexity of the signal, whereas, an increase in the Hurst exponent indicated a higher degree of correlation of the time series data with increasing UPDRS score from 0 to 3. The finding of gradual significant decrease for Hjorth parameters, maximum power, and total power reported in Table 14 support the clinical application of these parameters to quantify the levels of bradykinesia. Overall, classification accuracy provided in Table 15 shows that, a combination of the frequency features with nonlinear features can predict the severities of bradykinesia with high accuracy. The accuracy was about 10% higher than most recent works published on bradykinesia assessment which considered linear time domain parameters for its prediction system [3]. This can be justified by the notion that the classification was done selecting the features that are statistically significant. Also, the use of nonlinear features provided a new insight to reveal the underlying chaotic nature of highly complex signals like angular velocity signal of severe bradykinesia trial. Thus the results from this research utilizing the simulated data acquired from well-trained

participants known to emulate bradykinesia symptom to build a predictive system was well capable of scoring bradykinesia, the resulted accuracy was found to be satisfactory and ultimately facilitated us to develop the foundation of bradykinesia assessment system for PD patients.

In the second part of the bradykinesia assessment, data were collected from actual PD patients for finger tapping and hand grasping and the extracted features after signal processing of the data were tabulated in Table 16 and table 18. In the table, the green colors indicate that the feature values for before and after medication trend consistently with UPDRS scores obtained from the clinician before and after medication. As there were two types of task performed by patients: finger tapping and hand grasping, I would discuss about the effectiveness of our algorithm to quantify bradykinesia severity for these two types of task. From Table 16, we can see that no parameter trends consistently with the UPDRS scores for all the subjects. Sometimes people with high UPDRS scores has higher number of tapping with low amplitude of tapping. So the parameters vary from subject to subject. For Average opening velocity and closing velocity, there are 4 subjects for which change in parameter value after medication does not trend according with change or no change of UPDRS scores of PD patients after medication. At first we trained our machine learning classifier with the parameters: number of tapping, mean tap time, average closing acceleration, average opening angular velocity and average closing angular velocity. However with 5% cross validation performed on the trained classifier with the above mentioned parameters, Classification accuracy was 65.5%. Later standard deviation of tap time and hesitation was added to the feature list. As patients affected with PD bradykinesia tends to have variation in tapping time over the period of the task, we believed these features are effective to predict PD tremor. Cross validation accuracy when these two features are added to the list proves our hypothesis. As

shown in figure 16, prediction accuracy increased from 65.5% to 88.20% when number of tapping is decreased and standard deviation of tap time and hesitation parameter was included.

For hand grasping, 5 fold cross validation with four extracted features resulted into an accuracy of 64.3%. But similar to finger tapping, addition of two new features (standard deviation of grasp time and number of hesitation) improved the accuracy to 88.20%. Thus the analysis interpreted that the number of hesitation and the variation of the grasp time could be used as biomarkers for the assessment of bradykinesia of PD patients.

3.2.3 Gait

The gait quantification was done on three different database: first a speed on normal subjects, then on a database containing both PD patients and healthy matched controls and finally on a the sensor data collected by us from PD patients.

In the study of gait analysis with normal patients, we have proposed a Kalman filter based gait speed measurement algorithm from inertial measurement unit worn in top of a foot. Treadmill speed was used as reference for comparison of measured speed and actual speed. Calibrating the accelerometer sensor was essential preprocessing step for good measurement. For initial speed measurement before applying Kalman filter, Sabatini's algorithm of strap down integration method was simplified to extract gait velocity parameter ignoring other parameters [12]. Kalman filter was implemented to better estimate the gait speed. The optimization of noise covariance and weight matrices was done properly by trial and error method to remove the noise from the estimated instantaneous speed. The average mean squared errors for four sets of speeds were found to be 0.23, which indicates an acceptable estimation.

The performance of the system on four different speeds has confirmed the efficacy of the proposed method to estimate gait speed from inertial measurement unit. The improvement of

experimental results obtained by applying Kalman filter has verified the noise removal capability of Kalman filter for accurate estimation of gait speed. Though the outcome of the proposed study is appealing, there are several limitations. The algorithm only considers movement in sagittal plane, not in 3D plane. Again, instead of more accurate reference system, here treadmill was used as reference, which may not be quite accurate for proper speed measurement. Regardless of the limitations, the study proposes a gait speed measurement algorithm from inertial measurement unit with acceptable accuracy. This algorithm can be developed to use it for monitoring the progression of walking ability after various neurophysiological diseases like Parkinson's or strokes. A lot of research has been done to find an effective way of gait disturbance monitoring for patients suffering from Parkinson Disease [17]. Based on the results obtained in this study, it is possible to use inertial measurement data to identify the subsequent gait cycles and gait disorders by reliable estimation of walking speed on a treadmill.

Inspired from the findings of these two studies conducted by us, we have attached IMU sensors in the shoe of PD patients, collected the signal, analyzed the data and used a SVM based prediction model to predict the PD severity based on the features extracted from the signal.

For the clinical trial of PD patients 7 parameters were extracted from PD patients while all the parameters in theory should indicate PD gait disorder severity [91][50] However, variability and swing parameter does not trend accordingly in more than occasions. As classification accuracy of 85.2% achieved, so it can be said the combination of parameters can predict tremor severity can be adopted for home or remote monitoring of PD patients.

CHAPTER 4

CONCLUSION AND FUTURE WORK

4.1   Conclusion

The current work presents a comprehensive study highlighting the efficacy of different signal processing and machine learning techniques towards devising an accurate prediction system PD symptom assessment system using both simulated data and PD patient data acquired from IMU. Set of meaningful features that can correctly define the tremor, bradykinesia and gait were extracted from respective signals. The best prediction accuracy was obtained from the extracted features by testing SVM, random forest, kNN, and decision tree classifiers. The results demonstrated by the classification accuracy of tremor, bradykinesia and gait showed the effectiveness of the proposed approaches for all of these PD symptoms and highlights that the proposed signal processing and features-based machine learning approach has the potential for application in clinical diagnosis and longitudinal monitoring. The results of the current study also underscore the ability of the IMU data obtained non-invasively from wearable devices, in combination with a SVM classifier trained on meticulously selected features, as a tool for diagnosis of PD and monitoring effectiveness of therapy post pathology.

4.2 Future Work

In our future work, non-linear properties of PD symptoms will be analyzed, and fusion of non-linear and linear features will be investigated to see whether this leads to improvement in classification accuracy for PD diagnosis. Also, we will improve the system to make it more user friendly so that the symptom assessment technique can be implemented as a real time PD symptom monitoring system.

4.3 My Contribution

My contribution to this research was to develop an algorithm to process sensor signal, extract and analyze parameters from the signal and quantify different PD symptoms (Tremor, bradykinesia, gait) from the extracted features. As the result of research conducted in this thesis, the following journal and conference papers were published:

1. **Alam, M.N.,** Garg, A., Munia, T.T.K., Fazel-Rezai, R. and Tavakolian, K., 2017. Vertical ground reaction force marker for Parkinson's disease. PloS one, 12(5), p.e0175951.

2. **Md N Alam,** Tamanna T. K. Munia, Ajay K. Verma, Jau-Shin Lou, Collin Combs, Kouhyar Tavakolian, Reza Fazel-Rezai, "A Quantitative Assessment of Bradykinesia Using Initial Measurement Unit" 2017 Design of Medical Devices Conference, Minneapolis, Minnesota, USA, April 10–13, 2017, ISBN: 978-0-7918-4067-2.

3. **Alam, M.N.,** Tamanna T. K. Munia and Fazel-Rezai, R., 2017, July. Gait speed estimation using Kalman Filtering on inertial measurement unit data. In Engineering in Medicine and Biology Society (EMBC), 2017 39th Annual International Conference of the IEEE (pp. 2406-2409). IEEE.

4. **Alam, M.N.,** Johnson, B., Gendreau, J., Tavakolian, K., Combs, C. and Fazel-Rezai, R., 2016, May. Tremor quantification of Parkinson's disease-a pilot study. In *Electro Information Technology (EIT), 2016 IEEE International Conference on* (pp. 0755-0759). IEEE.

4.4   Other Contributions

1. **Alam, M.N.,** Munia, T.T.K., Tavakolian, K., Vasefi, F., MacKinnon, N. and Fazel-Rezai, R., 2016, August. Automatic detection and severity measurement of eczema using image processing. In *Engineering in Medicine and Biology Society (EMBC), 2016 IEEE 38th Annual International Conference of the* (pp. 1365-1368). IEEE.

2. Johnson, B., Erickson, J., Schneider, C., **Alam, M.N.,** Glessing, D., Wilson, N., Tavakolian, K. and Fazel-Rezai, R., 2016, May. Aviation navigation feedback device. In *Electro Information Technology (EIT), 2016 IEEE International Conference on* (pp. 0760-0764). IEEE.

BIBLIOGRAPHY

[1]   "Parkinson's Disease (PD)." [Online]. Available: https://www.mayfieldclinic.com/PE-PD.htm. [Accessed: 28-Oct-2017].

[2]   "Ageing and Parkinson's disease: Why is advancing age the biggest risk factor?," *Ageing Res. Rev.*, vol. 14, pp. 19–30, Mar. 2014.

[3]   "Parkinson's disease Symptoms - Mayo Clinic." [Online]. Available: https://www.mayoclinic.org/diseases-conditions/parkinsons-disease/basics/symptoms/con-20028488. [Accessed: 28-Oct-2017].

[4]   "Statistics on Parkinson's | Parkinson's Disease Foundation (PDF)." [Online]. Available: http://www.pdf.org/parkinson_statistics. [Accessed: 18-Jun-2017].

[5]   "Get Safe Homeopathic Treatment for Parkinson's Disease." [Online]. Available: http://www.sabeelhomeoclinic.com/parkinsons-disease-symptoms-causes-and-homeopathic-treatment.html. [Accessed: 19-Jun-2017].

[6]   P. Hickey and M. Stacy, "Available and emerging treatments for Parkinson's disease: a review.," *Drug Des. Devel. Ther.*, vol. 5, pp. 241–54, 2011.

[7]   "Parkinson's Disease Information Page | National Institute of Neurological Disorders and Stroke." [Online]. Available: https://www.ninds.nih.gov/Disorders/All-Disorders/Parkinsons-Disease-Information-Page. [Accessed: 28-Oct-2017].

[8]   F. Savery, "Amantadine and a fixed combination of levodopa and carbidopa in the treatment of Parkinson's disease.," *Dis. Nerv. Syst.*, vol. 38, no. 8, pp. 605–8, Aug. 1977.

[9]   "Deep brain stimulation - Overview - Mayo Clinic." [Online]. Available: https://www.mayoclinic.org/tests-procedures/deep-brain-stimulation/home/ovc-20156088. [Accessed: 28-Oct-2017].

[10]   "A Shocking Way to Fix the Brain - MIT Technology Review." [Online]. Available: https://www.technologyreview.com/s/542176/a-shocking-way-to-fix-the-brain/. [Accessed: 28-Oct-2017].

[11]   "Movement Symptoms." [Online]. Available: http://www.parkinson.org/Understanding-Parkinsons/Symptoms/Movement-Symptoms. [Accessed: 04-Nov-2017].

[12]   A. Salarian, H. Russmann, C. Wider, P. R. Burkhard, F. J. G. Vingerhoets, and K. Aminian, "Quantification of Tremor and Bradykinesia in Parkinson's Disease Using a Novel Ambulatory Monitoring System," *IEEE Trans. Biomed. Eng.*, vol. 54, no. 2, pp. 313–322, Feb. 2007.

[13]   L. Rubchinsky, A. Kuznetsov, V. MD, and K. Sigvardt, "Tremor," *Scholarpedia*, vol. 2, no. 10, p. 1379, 2007.

[14]   "At left, the patient exhibits tremor at rest, which, when accompanied by rigidity and bradykinesia, is typical of parkinsonian tremor. At right, a … | Pinteres…." [Online]. Available: https://www.pinterest.com/pin/430727151831617302/. [Accessed: 19-Jun-2017].

[15]   R. C. Helmich, M. J. R. Janssen, W. J. G. Oyen, B. R. Bloem, and I. Toni, "Pallidal dysfunction drives a cerebellothalamic circuit into Parkinson tremor," *Ann. Neurol.*, vol.

69, no. 2, pp. 269–281, Feb. 2011.

[16] M. Hallett, "Parkinson's disease tremor: pathophysiology," *Parkinsonism Relat. Disord.*, vol. 18, pp. S85–S86, Jan. 2012.

[17] M. Doder, E. A. Rabiner, N. Turjanski, A. J. Lees, D. J. Brooks, and 11C-WAY 100635 PET study, "Tremor in Parkinson's disease and serotonergic dysfunction: an 11C-WAY 100635 PET study.," *Neurology*, vol. 60, no. 4, pp. 601–5, Feb. 2003.

[18] F. Magrinelli *et al.*, "Pathophysiology of Motor Dysfunction in Parkinson's Disease as the Rationale for Drug Treatment and Rehabilitation," *Parkinsons. Dis.*, vol. 2016, pp. 1–18, Jun. 2016.

[19] R. L. Albin, A. B. Young, and J. B. Penney, "The functional anatomy of basal ganglia disorders.," *Trends Neurosci.*, vol. 12, no. 10, pp. 366–75, Oct. 1989.

[20] M. R. DeLong, "Primate models of movement disorders of basal ganglia origin," *Trends Neurosci.*, vol. 13, no. 7, pp. 281–285, 1990.

[21] J. P. Dick *et al.*, "The Bereitschaftspotential is abnormal in Parkinson's disease.," *Brain*, pp. 233–44, Feb. 1989.

[22] M. Picillo, G. B. Vincos, D. S. Kern, S. H. Fox, A. E. Lang, and A. Fasano, "Learning More from Finger Tapping in Parkinson's Disease: Up and Down from Dyskinesia to Bradykinesia," *Mov. Disord. Clin. Pract.*, vol. 3, no. 2, pp. 184–187, Mar. 2016.

[23] H. Dai, H. Lin, and T. C. Lueth, "Quantitative assessment of parkinsonian bradykinesia based on an inertial measurement unit," *Biomed. Eng. Online*, vol. 14, no. 1, p. 68, Dec. 2015.

[24] B. R. Bloem, J. M. Hausdorff, J. E. Visser, and N. Giladi, "Falls and freezing of gait in Parkinson's disease: A review of two interconnected, episodic phenomena," *Mov. Disord.*, vol. 19, no. 8, pp. 871–884, Aug. 2004.

[25] N. Giladi, F. B. Horak, and J. M. Hausdorff, "Classification of gait disturbances: distinguishing between continuous and episodic changes.," *Mov. Disord.*, vol. 28, no. 11, pp. 1469–73, Sep. 2013.

[26] D. Domkin *et al.*, "Joint angle variability in 3D bimanual pointing: uncontrolled manifold analysis," *Exp. Brain Res.*, vol. 163, no. 1, pp. 44–57, May 2005.

[27] "Parkinson's disease – NewsMD: What's Hot in Health." [Online]. Available: https://mariadorfner.wordpress.com/tag/parkinsons-disease/. [Accessed: 19-Jun-2017].

[28] "IMU and INS - VectorNav Library." [Online]. Available: https://www.vectornav.com/support/library/imu-and-ins. [Accessed: 31-Oct-2017].

[29] "Inertial measurement unit - Wikipedia." [Online]. Available: https://en.wikipedia.org/wiki/Inertial_measurement_unit. [Accessed: 31-Oct-2017].

[30] S. Du, W. Sun, and Y. Gao, "MEMS IMU Error Mitigation Using Rotation Modulation Technique," *Sensors*, vol. 16, no. 12, p. 2017, Nov. 2016.

[31] "Sparks N Smoke: 69. The Sense HAT's Inertial Measurement Unit." [Online]. Available: http://smokespark.blogspot.com/2015/10/69-sense-hat-using-inertial-measurement.html. [Accessed: 19-Jun-2017].

[32] F. M. Khan, M. Barnathan, M. Montgomery, S. Myers, L. Cote, and S. Loftus, "A Wearable Accelerometer System for Unobtrusive Monitoring of Parkinson's Diease Motor Symptoms," in *2014 IEEE International Conference on Bioinformatics and Bioengineering*, 2014, pp. 120–125.

[33] "Accelerometer and Gyroscopes Sensors: Operation, Sensing, and Applications - Application Note - Maxim." [Online]. Available: https://www.maximintegrated.com/en/app-notes/index.mvp/id/5830. [Accessed: 31-Oct-2017].

[34] "Accelerometers: What They Are & How They Work." [Online]. Available: https://www.livescience.com/40102-accelerometers.html. [Accessed: 31-Oct-2017].

[35] "Gyroscope," *Oxford Dictionaries*.

[36] C. G. Goetz *et al.*, "Movement Disorder Society-sponsored revision of the Unified Parkinson's Disease Rating Scale (MDS-UPDRS): Scale presentation and clinimetric testing results," *Mov. Disord.*, vol. 23, no. 15, pp. 2129–2170, Nov. 2008.

[37] G. Geminiani *et al.*, "Interobserver reliability between neurologists in training of Parkinson's disease rating scales. A multicenter study," *Mov. Disord.*, vol. 6, no. 4, pp. 330–335, 1991.

[38] M. Richards, K. Marder, L. Cote, and R. Mayeux, "Interrater reliability of the unified Parkinson's disease rating scale motor examination," *Mov. Disord.*, vol. 9, no. 1, pp. 89–91, Jan. 1994.

[39] M. Bacher, E. Scholz, and H. C. Diener, "24 Hour continuous tremor quantification based on EMG recording," *Electroencephalogr. Clin. Neurophysiol.*, vol. 72, no. 2, pp. 176–183, 1989.

[40] P. E. O'Suilleabhain and R. B. Dewey, "Validation for tremor quantification of an electromagnetic tracking device.," *Mov. Disord.*, vol. 16, no. 2, pp. 265–71, Mar. 2001.

[41] K. E. Norman, R. Edwards, and A. Beuter, "The measurement of tremor using a velocity transducer: comparison to simultaneous recordings using transducers of displacement, acceleration and muscle activity.," *J. Neurosci. Methods*, vol. 92, no. 1–2, pp. 41–54, Oct. 1999.

[42] K. Niazmand, K. Tonn, A. Kalaras, U. M. Fietzek, J. H. Mehrkens, and T. C. Lueth, "Quantitative evaluation of Parkinson's disease using sensor based smart glove," in *2011 24th International Symposium on Computer-Based Medical Systems (CBMS)*, 2011, pp. 1–8.

[43] P. R. Burkhard, H. Shale, J. W. Langston, and J. W. Tetrud, "Quantification of dyskinesia in Parkinson's disease: validation of a novel instrumental method.," *Mov. Disord.*, vol. 14, no. 5, pp. 754–63, Sep. 1999.

[44] P. Pierleoni, L. Palma, A. Belli, and L. Pernini, "A real-time system to aid clinical classification and quantification of tremor in Parkinson's disease," in *IEEE-EMBS International Conference on Biomedical and Health Informatics (BHI)*, 2014, pp. 113–116.

[45] Honghua Zhang, Xiaoyu Chen, Wen-Yen Lin, Wen-Cheng Chou, and Ming-Yih Lee, "A novel accelerometer-based method for the real-time assessment of Parkinson's tremor," in

2014 IEEE International Conference on Communiction Problem-solving, 2014, pp. 87–90.

[46]   H. Jeon *et al.*, "Automatic Classification of Tremor Severity in Parkinson's Disease Using a Wearable Device," *Sensors*, vol. 17, no. 9, p. 2067, Sep. 2017.

[47]   J. P. Giuffrida, D. E. Riley, B. N. Maddux, and D. A. Heldman, "Clinically deployable Kinesia^{TM} technology for automated tremor assessment," *Mov. Disord.*, vol. 24, no. 5, pp. 723–730, Apr. 2009.

[48]   O. Martinez-Manzanera, E. Roosma, M. Beudel, R. W. K. Borgemeester, T. van Laar, and N. M. Maurits, "A Method for Automatic and Objective Scoring of Bradykinesia Using Orientation Sensors and Classification Algorithms," *IEEE Trans. Biomed. Eng.*, vol. 63, no. 5, pp. 1016–1024, May 2016.

[49]   J.-W. Kim *et al.*, "Quantification of bradykinesia during clinical finger taps using a gyrosensor in patients with Parkinson?s disease," *Med. Biol. Eng. Comput.*, vol. 49, no. 3, pp. 365–371, Mar. 2011.

[50]   D. A. Heldman *et al.*, "Automated motion sensor quantification of gait and lower extremity bradykinesia," in *2012 Annual International Conference of the IEEE Engineering in Medicine and Biology Society*, 2012, vol. 2012, pp. 1956–1959.

[51]   D. A. Heldman *et al.*, "The modified bradykinesia rating scale for Parkinson's disease: reliability and comparison with kinematic measures.," *Mov. Disord.*, vol. 26, no. 10, pp. 1859–63, Aug. 2011.

[52]   B. P. Printy *et al.*, "Smartphone application for classification of motor impairment severity in Parkinson's disease," in *2014 36th Annual International Conference of the IEEE Engineering in Medicine and Biology Society*, 2014, pp. 2686–2689.

[53]   R. J. Dunnewold, C. E. Jacobi, and J. J. van Hilten, "Quantitative assessment of bradykinesia in patients with Parkinson's disease.," *J. Neurosci. Methods*, vol. 74, no. 1, pp. 107–12, Jun. 1997.

[54]   D. G. M. Zwartjes, T. Heida, J. P. P. van Vugt, J. A. G. Geelen, and P. H. Veltink, "Ambulatory Monitoring of Activities and Motor Symptoms in Parkinson's Disease," *IEEE Trans. Biomed. Eng.*, vol. 57, no. 11, pp. 2778–2786, Nov. 2010.

[55]   G. Pal and C. G. Goetz, "Assessing bradykinesia in parkinsonian disorders.," *Front. Neurol.*, vol. 4, p. 54, 2013.

[56]   S. Mudge and N. S. Stott, "Outcome measures to assess walking ability following stroke: a systematic review of the literature," *Physiotherapy*, vol. 93, no. 3, pp. 189–200, Sep. 2007.

[57]   P. J. Friedman, D. E. Richmond, and J. J. Baskett, "A prospective trial of serial gait speed as a measure of rehabilitation in the elderly.," *Age Ageing*, vol. 17, no. 4, pp. 227–35, Jul. 1988.

[58]   S. Mihradi, Ferryanto, T. Dirgantara, and A. I. Mahyuddin, "Development of an optical motion-capture system for 3D gait analysis," in *2011 2nd International Conference on Instrumentation, Communications, Information Technology, and Biomedical Engineering*, 2011, pp. 391–394.

[59] S. Frenkel-Toledo, N. Giladi, C. Peretz, T. Herman, L. Gruendlinger, and J. M. Hausdorff, "Treadmill walking as an external pacemaker to improve gait rhythm and stability in Parkinson's disease," *Mov. Disord.*, vol. 20, no. 9, pp. 1109–1114, Sep. 2005.

[60] J. M. Hausdorff, J. Balash, and N. Giladi, "Effects of Cognitive Challenge on Gait Variability in Patients with Parkinson?s Disease," *J. Geriatr. Psychiatry Neurol.*, vol. 16, no. 1, pp. 53–58, Mar. 2003.

[61] S. Bamberg, A. Y. Benbasat, D. M. Scarborough, D. E. Krebs, and J. A. Paradiso, "Gait Analysis Using a Shoe-Integrated Wireless Sensor System," *IEEE Trans. Inf. Technol. Biomed.*, vol. 12, no. 4, pp. 413–423, Jul. 2008.

[62] J. Barth *et al.*, "Stride Segmentation during Free Walk Movements Using Multi-Dimensional Subsequence Dynamic Time Warping on Inertial Sensor Data," *Sensors*, vol. 15, no. 3, pp. 6419–6440, Mar. 2015.

[63] M. Demonceau *et al.*, "Contribution of a Trunk Accelerometer System to the Characterization of Gait in Patients With Mild-to-Moderate Parkinson's Disease," *IEEE J. Biomed. Heal. Informatics*, vol. 19, no. 6, pp. 1803–1808, Nov. 2015.

[64] K. Aminian, P. Robert, E. Jequier, and Y. Schutz, "Estimation of speed and incline of walking using neural network," in *Conference Proceedings. 10th Anniversary. IMTC/94. Advanced Technologies in I & M. 1994 IEEE Instrumentation and Measurement Technolgy Conference (Cat. No.94CH3424-9)*, pp. 160–162.

[65] S. Miyazaki, "Long-term unrestrained measurement of stride length and walking velocity utilizing a piezoelectric gyroscope," *IEEE Trans. Biomed. Eng.*, vol. 44, no. 8, pp. 753–759, Aug. 1997.

[66] K. Tong and M. H. Granat, "A practical gait analysis system using gyroscopes," *Med. Eng. Phys.*, vol. 21, no. 2, pp. 87–94, Mar. 1999.

[67] A. M. Sabatini, C. Martelloni, S. Scapellato, and F. Cavallo, "Assessment of Walking Features From Foot Inertial Sensing," *IEEE Trans. Biomed. Eng.*, vol. 52, no. 3, pp. 486–494, Mar. 2005.

[68] J. C. Alvarez, R. C. Gonzalez, D. Alvarez, A. M. Lopez, and J. Rodriguez-Uria, "Multisensor Approach to Walking Distance Estimation with Foot Inertial Sensing," in *2007 29th Annual International Conference of the IEEE Engineering in Medicine and Biology Society*, 2007, pp. 5719–5722.

[69] R. Baltadjieva, N. Giladi, L. Gruendlinger, C. Peretz, and J. M. Hausdorff, "Marked alterations in the gait timing and rhythmicity of patients with *de novo* Parkinson's disease," *Eur. J. Neurosci.*, vol. 24, no. 6, pp. 1815–1820, Sep. 2006.

[70] J. M. Hausdorff, "Stride variability: beyond length and frequency," *Gait Posture*, vol. 20, no. 3, p. 304, Dec. 2004.

[71] M. E. Feltner, P. G. MacRae, and J. L. McNitt-Gray, "Quantitative gait assessment as a predictor of prospective and retrospective falls in community-dwelling older women.," *Arch. Phys. Med. Rehabil.*, vol. 75, no. 4, pp. 447–53, Apr. 1994.

[72] J. M. Hausdorff, D. A. Rios, and H. K. Edelberg, "Gait variability and fall risk in community-living older adults: A 1-year prospective study," *Arch. Phys. Med. Rehabil.*, vol. 82, no. 8, pp. 1050–1056, Aug. 2001.

[73] S. V. Perumal and R. Sankar, "Gait and tremor assessment for patients with Parkinson's disease using wearable sensors," *ICT Express*, vol. 2, no. 4, pp. 168–174, Dec. 2016.

[74] J. R. Hughes *et al.*, "Parkinsonian abnormality of foot strike: a phenomenon of ageing and/or one responsive to levodopa therapy?," *Br. J. Clin. Pharmacol.*, vol. 29, no. 2, pp. 179–86, Feb. 1990.

[75] L. Palmerini, L. Rocchi, S. Mazilu, E. Gazit, J. M. Hausdorff, and L. Chiari, "Identification of Characteristic Motor Patterns Preceding Freezing of Gait in Parkinson's Disease Using Wearable Sensors," *Front. Neurol.*, vol. 8, p. 394, Aug. 2017.

[76] M. P. Murray, S. B. Sepic, G. M. Gardner, and W. J. Downs, "Walking patterns of men with parkinsonism.," *Am. J. Phys. Med.*, vol. 57, no. 6, pp. 278–94, Dec. 1978.

[77] S. Kimmeskamp and E. M. Hennig, "Heel to toe motion characteristics in Parkinson patients during free walking.," *Clin. Biomech. (Bristol, Avon)*, vol. 16, no. 9, pp. 806–12, Nov. 2001.

[78] "MDS Rating Scales." [Online]. Available: http://www.movementdisorders.org/MDS/Education/Rating-Scales.htm. [Accessed: 18-Jun-2017].

[79] "User Manual and Specifications," 2015.

[80] T. Heida, E. Wentink, and E. Marani, "Power spectral density analysis of physiological, rest and action tremor in Parkinson's disease patients treated with deep brain stimulation," *J. Neuroeng. Rehabil.*, vol. 10, no. 1, p. 70, Jul. 2013.

[81] "Detrending Data - MATLAB & Simulink." [Online]. Available: https://www.mathworks.com/help/matlab/data_analysis/detrending-data.html?requestedDomain=www.mathworks.com. [Accessed: 28-Oct-2017].

[82] "1-D median filtering - MATLAB medfilt1." [Online]. Available: https://www.mathworks.com/help/signal/ref/medfilt1.html. [Accessed: 28-Oct-2017].

[83] "Welch's power spectral density estimate - MATLAB pwelch." [Online]. Available: https://www.mathworks.com/help/signal/ref/pwelch.html. [Accessed: 28-Oct-2017].

[84] "Gait Up | Make Sense of Motion." [Online]. Available: https://www.gaitup.com/. [Accessed: 28-Oct-2017].

[85] G. Welch and G. Bishop, "An Introduction to the Kalman Filter," 2006.

[86] "Support Vector Machine." [Online]. Available: https://en.wikipedia.org/wiki/Support_vector_machine. [Accessed: 16-May-2016].

[87] T. Cover and P. Hart, "Nearest neighbor pattern classification," *IEEE Trans. Inf. Theory*, vol. 13, no. 1, pp. 21–27, 1967.

[88] H. A. Simon, E. B. Hunt, J. Marin, and P. Stone, "Experiments in Induction," *Am. J. Psychol.*, vol. 80, no. 4, p. 651, Dec. 1967.

[89] I. Kononenko, "Estimating attributes: Analysis and extensions of RELIEF," Springer Berlin Heidelberg, 1994, pp. 171–182.

[90] A. Jovic and N. Bogunovic, "Random Forest-Based Classification of Heart Rate Variability Signals by Using Combinations of Linear and Nonlinear Features."

[91] B. Mariani, H. Rouhani, X. Crevoisier, and K. Aminian, "Quantitative estimation of foot-flat and stance phase of gait using foot-worn inertial sensors.," *Gait Posture*, vol. 37, no. 2, pp. 229–34, Feb. 2013.